

27 distributed in the whole cell of fathead minnow (FHM) cells. Thus, the N-terminate signal peptide
28 had a significant impact on mitochondrial targeting. Notably, the expression of ORF3141 protein
29 changed the distribution of mitochondria from perinuclear halo into lumps in the transfected FHM
30 cells. In addition, apoptotic features were found in the transfected FHM cells by overexpression of
31 ORF3141 and ORF3141 Δ sig proteins, respectively. Quantitative assays of mitochondrial membrane
32 potential value, caspase-3 activity and apoptosis-related gene mRNA expression suggested that cell
33 apoptosis was induced in the transfected FHM cells. In conclusion, the ORF3141 was a secreted
34 protein of *N. seriolae* that targeted host cell mitochondria and induced apoptosis in FHM cells. This
35 protein may participate in the cell apoptosis regulation and plays an important role in the
36 pathogenesis of *N. seriolae*.

37 **Keywords:** *Nocardia seriolae*; secreted protein; subcellular localization; mitochondrial targeting;
38 cell apoptosis

39 **Author summary**

40 *Nocardia seriolae* is the causative pathogen responsible for fish nocardiosis. This facultative
41 intercellular bacterium, adapts to survive and colonize by evading intracellular killing after being
42 engulfed with macrophages in the host. Despite considerable economic losses caused by *N.*
43 *seriolae* in fish infection, the pathogenic mechanism and specific virulence factor of this bacterium
44 remain ambiguous. In this study, the characteristic of ORF3141 protein function was investigated
45 by subcellular localization and its possible contributions on the ability of *N. seriolae* to induce
46 apoptosis in transfected fathead minnow (FHM) cells was investigated. Here, we confirmed that
47 ORF3141 was a secreted protein that targeted host cell mitochondria and induced cell apoptosis in
48 FHM cells. Interestingly, after deleting the signal peptide, ORF3141 Δ sig protein was evenly
49 distributed in the whole host cell and did not co-localize with the mitochondria which could also
50 induce cell apoptosis. Thus, the N-terminate signal peptide played an important role in
51 mitochondrial targeting, and the domain part without the signal peptide had a critical relationship
52 with cell apoptosis. These results demonstrated that ORF3141 may act as a potential virulence
53 factor that induces apoptosis in fish cells. This protein is significant to elucidate the pathogenic

54 mechanism of *N. seriolae* and this study may provide beneficial insight to prevent and treat fish
55 nocardiosis.

56 **Introduction**

57 Fish nocardiosis is a systemic bacterial disease with three kinds of pathogenic bacteria, namely,
58 *Nocardia seriolae*, *N. samonocida* and *N. asteroides*, which have been isolated from diseased fish [1–
59 3]. The outbreak of fish nocardiosis is frequently reported in global aquaculture industries and has
60 caused substantial commercial losses in Southeast Asia, especially China [4–7]. However, the
61 pathogen of fish nocardiosis that has been reported with considerable frequency is *N. seriolae*.
62 Notably, *N. seriolae* is the most frequently isolated *Nocardia sp.* from diseased fish [7]. This
63 bacterium is an opportunistic pathogen, by infecting immunocompromised fishes through feeds,
64 gills, and wounds and causing chronic systemic granulomatous disease [8]. The clinical signs of
65 infected fish include skin ulcers and numerous white nodular structures on the gills and in the head
66 kidney, trunk kidney, spleen, and liver [9]. *N. seriolae* infections have been documented in more
67 than 39 kinds of fish, both freshwater and especially marine species, such as golden pompano
68 (*Trachinotus ovatus*), snubnose pompano (*T. blochii*), yellow croaker (*Larimichthys crocea*),
69 northern snakehead (*Channa argus*), blotched snakehead (*C. maculata*), largemouth bass
70 (*Micropterus salmoides*), yellow tail (*Seriola quinqueradiata*), amberjack (*S. dumerelli*) and sea
71 bass (*Lateolabrax japonicus*) [5,10,11].

72 The pathogenic mechanisms and specific virulence factor of *N. seriolae* remain unknown.
73 Beaman found that the virulence of *N. asteroides* was associated with its resistance to oxidative
74 killing by phagocytes, inhibition of phagosome-lysosome fusion, neutralization of phagosomal
75 acidification, and alteration of lysosomal enzymes within phagocytes, as well as the secretion of
76 toxic substances by the nocardia, which are apparently involved in these processes [12]. Previous
77 studies showed that *N. asteroides* might induce apoptosis in host cells [13–15]. The secretome
78 studies of pathogenic actinomycetes have shown that secreted proteins, especially several
79 mitochondrial targeted proteins, are closely related to their pathogenicity and may play an important
80 role in the regulation of cell apoptosis and bacterial pathogenesis [16–19]. The modulation of cell

81 apoptosis in the host by pathogenic bacteria is a major pathogenicity mechanism. Many bacterial
82 proteins have a highly specific activity with the host mitochondria, which participate in the cell
83 apoptosis by influencing the signaling pathways [20–22]. The mechanism of mitochondrial pathway
84 regulation of apoptosis is very complex. The mitochondrial targeted protein allows the
85 mitochondrial outer membrane permeabilization (MOMP) accompanied with the loss of
86 mitochondrial membrane potential ($\Delta\Psi_m$). Subsequently, various apoptotic mediators (mammalian
87 serine protease (Omi/HtrA2), second mitochondrial activator of caspase (SMAC), direct IAP
88 binding protein with low pI (Diablo), cytochrome C (Cyt C), and apoptosis-inducing factors (AIF))
89 are released into the cytosol. The releases of Cyt c in cytosol causes the association of apoptosis
90 protease-activating factor-1 (Apaf-1) and ATP/dATP to form apoptotic body, while AIF enters the
91 nucleus acting in a caspase independent manner by causing chromatin condensation and
92 fragmentation. Finally, the downstream procaspase-3 is activated, and cell apoptosis is induced in
93 the host [23–25]. Thus, we speculated whether the mitochondrial targeting secreted proteins from
94 *N. seriolae* are potential virulence factors.

95 A bioinformatic analysis based on the whole genome sequence data of *N. seriolae* strain
96 ZJ0503 [26] showed that *ORF3141* encoded a secreted protein which might target the mitochondria
97 in the host cell, and the ORF3141 protein had a signal peptide at the N-terminate (residues 1-30,
98 MKLLNPRGFGLVCASAAVAAGLMLAGCANT). Currently, the function of this protein and its
99 homologs are totally unknown. Meanwhile, the homologs of ORF3141 are mainly present in high
100 GC Gram-positive bacteria. We proposed that the secreted protein of ORF3141 was possibly a
101 virulence factor of *N. seriolae* strain ZJ0503. In this study, the function of ORF3141 was explored
102 and whether this protein was the bacterial virulence factor that induced infection in fish was
103 determined. Gene cloning, secreted protein identification, subcellular localization, overexpression,
104 and apoptosis detection assays of ORF3141 and ORF3141 Δ sig proteins were performed. Moreover,
105 the results indicated that *ORF3141* gene encoded a secreted protein which contained a mitochondrial
106 targeting sequence was and involved in apoptosis regulation. These results may lay the foundation
107 for further study on the function of ORF3141 protein and promote the understanding of the
108 molecular pathogenic mechanism of *N. seriolae*.

109 **Results**

110 **Cloning and the sequence analysis of ORF3141**

111 The *ORF3141* and *ORF3141* Δ *sig* genes of *N. seriolae* strain ZJ0503 were cloned, and the
112 recombinant plasmids of pEGFP-3141, pEGFP-3141 Δ *sig*, pcDNA-3141, and pcDNA-3141 Δ *sig*
113 were constructed successfully. Sequence analysis revealed that an open reading frame (ORF) of
114 *ORF3141* gene was 558 bp, and the deduced amino acid sequence had a length of 185 residues (Fig.
115 1A). The predicted molecular weight of ORF3141 protein was 18.96 kDa, and the theoretical
116 isoelectric point (pI) was 5.85. The instability index of ORF3141 was computed to be 25.43,
117 indicating its stability. The grand average of hydropathicity was -0.112, which signifies that the
118 ORF3141 protein was hydrophilic. ORF3141 was predicted to be a secreted protein with a cleavable
119 signal peptide at N-terminus and co-localized with the mitochondria in the host. ORF3141 was
120 composed of a signal peptide (residues 1-30, MKLLNPRGFGLVCASAAVAAGLMLAGCANT)
121 at N-terminate, two low complexity domains (residues 47-70 and 90-117), and five kinds of
122 functional sites including N-myristoylation, Protein kinase C phosphorylation, Casein kinase II
123 phosphorylation, N-glycosylation, and cAMP- and cGMP-dependent protein kinase
124 phosphorylation sites (Fig. 1B). No protein superfamily members of ORF3141 protein were found.
125 The three-dimensional structure of ORF3141 from *N. seriolae* was predicted by I-TASSER. The
126 structure was closed to that of multidrug ABC transporter Sav1866 from *Staphylococcus aureus*
127 (Fig. 1C), which was classified as a hydrolase [27]. Moreover, the protein contained two ligand
128 binding sites (residues 108 and 111) of coenzyme F430 and an enzyme active site (residues 107) of
129 ATP phosphohydrolase (steroid-exporting).

130 Protein BLAST showed that the deduced amino acid sequence of ORF3141 protein displayed
131 low identity with homologous sequence from Actinomycetes, with the highest identity of *N.*
132 *concava* (84%) and the lowest identity of *Mycobacterium marinum* (23%). This protein had a rather
133 high homology in *Nocardia* species (61% - 84%) (S1 Table) and its sequence was also found in
134 other *N. seriolae* stains, such as *N. seriolae* N-2927 [28], *N. seriolae* U-1 [29], *N. seriolae*
135 EM150506, *N. seriolae* CK-14008 and *N. seriolae* UTF-1 [30] (S2 Table). Multiple alignment of
136 the deduced amino acid sequences of the ORF3141 protein showed no putative conserved domains

137 (Fig. 2A). A phylogenetic tree was constructed to identify the evolutionary relationships between
138 *N. seriolae* with other species of ORF3141 homologs, on the basis of the deduced amino acid
139 sequence of ORF3141. The results showed that ORF3141 proteins in *Nocardia sp.* were clustered in
140 one group (Fig. 2B).

141 **Identification of ORF3141 protein was a secreted protein**

142 Preparation and shotgun mass spectrometry (MS) of the extracellular products of *N. seriolae*
143 strain ZJ0503 showed that the characteristic peptide “TIETELNATR” of ORF3141 was detected
144 with confidence greater than or equal to 99%. This result confirmed that ORF3141 was a secreted
145 protein of *N. seriolae*.

146 **Subcellular localization of ORF3141 and ORF3141 Δ sig proteins in FHM cells**

147 Subcellular localization of ORF3141 and ORF3141 Δ sig proteins in the FHM cells were
148 determined by the expression of ORF3141-GFP and ORF3141 Δ sig-GFP fusion protein,
149 respectively. ORF3141-GFP and ORF3141 Δ sig-GFP fusion protein were detected with strong
150 green fluorescence signal at 48 h post-transfection (hpt). The mitochondria were shown with red
151 fluorescence, and the nucleus were displayed with blue fluorescence. Compared with the location
152 of mitochondria and nucleus in the pEGFP-3141 or pEGFP-3141 Δ sig transfected cells, the
153 ORF3141-GFP fusion protein was exhibited an aggregated distribution and co-localized with the
154 mitochondria in the cytoplasm, while the ORF3141 Δ sig-GFP fusion protein was distributed in the
155 whole FHM cell and did not co-localize with the mitochondria. These contrasting results indicated
156 that the N-terminate signal peptide played an important role in mitochondrial targeting. In addition,
157 the expression of ORF3141 or ORF3141 Δ sig proteins changed the distribution of the mitochondria
158 from perinuclear halo into lumps, and the apoptotic bodies were detected. By contrast, the signal of
159 GFP was distributed in both cytoplasm and nucleus in the control cells which were transfected with
160 pEGFP-N1, and no specific fluorescence co-localized with the mitochondria (Fig. 3).

161 **Apoptosis induced in FHM cells by overexpression of ORF3141 and ORF3141 Δ sig**
162 **proteins**

163 To investigate whether ORF3141 and ORF3141 Δ sig proteins were involved in the apoptosis
164 of fish cells, plasmids pcDNA-3141 and pcDNA-3141 Δ sig were transfected into the FHM cells,
165 respectively. Several typical apoptotic features, such as cellular shrinkage, blebbing of the nuclear
166 membrane, nuclear pyrosis, and nuclear fragmentation, in ORF3141 and ORF3141 Δ sig proteins
167 overexpressed FHM cells were observed by microscope with fluorescent and white light (Fig. 4).
168 Thus, the ORF3141 and ORF3141 Δ sig proteins might lead to fish cell apoptosis. The number of
169 apoptotic bodies were counted and used to calculate the apoptotic rate (number of apoptotic bodies
170 / total number of cells \times 100%) [31]. The results showed that 19.82 % and 17.05% cells underwent
171 apoptosis in pcDNA-3141 and pcDNA-3141 Δ sig transfected groups respectively, while only 2.75%
172 cells in control group (Fig. 5A). At 48 hpt, the expression of ORF3141 or ORF3141 Δ sig proteins
173 in the plasmids transfected FHM cells were confirmed by the presence of a specific band using RT-
174 PCR (Fig. 5B) and Western blot analysis (Fig. 5C).

175 **Apoptotic detection of ORF3141 and ORF3141 Δ sig overexpressed FHM cells**

176 The $\Delta\Psi_m$ was shown with the evident damage in JC-1 polymer/monomer fluorescence ratio in
177 ORF3141 or ORF3141 Δ sig overexpressed cells. The $\Delta\Psi_m$ values of both pcDNA-3141 and
178 pcDNA-3141 Δ sig transfected groups cells were decreased to minimum values at 72 hpt, which were
179 0.54- and 0.53-folds lower than that of the control cell group, respectively (Fig. 6A). Meanwhile,
180 measurement of caspase-3 activity showed that caspase-3 was activated in ORF3141 or
181 ORF3141 Δ sig proteins overexpressed cells and reached maximum value at 48 hpt, which were
182 approximately 1.23- and 1.80-folds higher than that of the control cell group, respectively (Fig. 6B).
183 Several apoptosis-related genes of Bcl-2 family mRNA expression were investigated at 0, 24, 48,
184 72, and 96 hpt by qRT-PCR, including B cell lymphoma-2 (*Bcl-2*), Bcl-2 associated X (*Bax*), Bcl-
185 2 antagonist of cell death (*Bad*), and Bcl-2 interacting domain death agonist (*Bid*) genes. The results
186 showed that pro-apoptotic (*Bad*, *Bid*, and *Bax*) and anti-apoptotic (*Bcl-2*) genes were rapidly
187 activated in both pcDNA-3141 and pcDNA-3141 Δ sig transfected groups cells and their mRNA
188 expression reached peak level at 72 hpt, respectively. Moreover, there were 11.19- and 10.60-folds

189 of *Bax* to *Bcl-2* genes mRNA expression in pcDNA-3141 and pcDNA-3141 Δ sig transfected groups
190 higher than that of 5.17-fold in the control group at 72 hpt (Fig. 6C). All quantitative assays of $\Delta\Psi_m$
191 value, caspase-3 activity, and apoptosis-related genes mRNA expression indicated that cell
192 apoptosis could be induced by the overexpression of ORF3141 or ORF3141 Δ sig proteins in the
193 FHM cells.

194 Discussion

195 No relevant literature on the ORF3141 protein of *Nocardia* or other species is available, and this
196 protein remains largely unknown. Here, we preliminary investigated the characteristic, structure,
197 and function of ORF3141 from *N. seriolae* strain ZJ0503. Moreover, *ORF3141* and *ORF3141* Δ sig
198 were successfully cloned. The sequence analysis showed an ORF of *ORF3141* gene of 558 bp. This
199 gene encoded a protein with 185 amino acid residues, molecular weight of 18.96 kDa, and isoelectric
200 point of 5.85. A phylogenetic tree based on the deduced amino acid sequence of ORF3141 shared
201 low homology between *N. seriolae* and other homologous sequences from Actinomycetes. However,
202 ORF3141 had a rather high homology in *Nocardia* species. Bioinformatic analysis revealed that
203 ORF3141 had no putative conserved domains and no superfamily. This protein comprised a signal
204 peptide and two low complexity domains, but the function of these domains remains unknown.
205 *ORF3141* was predicted to encode a secreted protein and co-localized with the mitochondria in the
206 host cells. Experimentally, the MS analysis of the extracellular products from *N. seriolae* strain
207 ZJ0503 proved that ORF3141 was a secreted protein. Subcellular localization of ORF3141 in the
208 host cells exhibited an aggregated distribution and coincided with the mitochondria. Thus, ORF3141
209 co-localized with the mitochondria in the host cells. Distinguishingly, ORF3141 Δ sig protein was
210 evenly distributed in the whole cell and did not co-localize with the mitochondria in the host cells.
211 These contrasting results were due to the presence or absence of the signal peptide. Similar results
212 were found in the subcellular localization study of EGFP-GRP75 fusion proteins; that is, GRP-75
213 with signal peptide was exclusively co-localized with the mitochondria, whereas GRP-75 without
214 the signal peptide was distributed in the whole host cell [32]. Thus, the N-terminate signal peptide
215 was important for mitochondrial targeting. The mitochondrial targeting protein contains specific

216 sequences with specific information. Five kinds of mitochondrial targeting signals (MTSs) are used
217 to determine the protein localization with the mitochondrial outer membranes, inner membranes, or
218 matrix [33]. Many proteins are destined for the mitochondrial matrix typically cleavable targeting
219 signal at the N-terminus [34], which are commonly 20 - 60 amino acids in length and are cleaved
220 upon import into the mitochondrial matrix by the mitochondrial processing peptidase [35,36].
221 Therefore, ORF3141 was assumed to target the mitochondria matrix.

222 The function of ORF3141 has not been studied, until now. In our study, we observed that the
223 distribution of mitochondria was altered from perinuclear halo into lumps, and apoptotic bodies
224 appeared during the subcellular localization and overexpression assays, which indicated that cell
225 apoptosis was induced after ORF3141 or ORF3141 Δ sig proteins stimulating in FHM cells.
226 Mitochondria appear to play a central role in the regulation of several cell death pathways, such as
227 apoptosis, autophagic cell death, necrosis, pyroptosis, and pyronecrosis [37,38]. Other characterized
228 bacterial proteins had also been shown to target the mitochondria and induce apoptosis. For example,
229 Omp38 of *Acinetobacter baumannii* was shown to target mitochondria of Hep-2 cells where it
230 induced the release of Cyt c and AIF, to promote apoptosis [39]. When expressed in human cells,
231 PorB of *Neisseria gonorrhoeae* co-localized with the mitochondria and caused dissipation of $\Delta\Psi_m$
232 but did not induce the release of Cyt c [40]. SipB of *Salmonella enterica* targeted the host cell
233 mitochondria during infection and supported autophagy-mediated cell death in caspase-1 deficient
234 macrophages [41]. As a mitochondrial targeting bacterial secreted protein, ORF3141 might
235 participate in the regulation of cell apoptosis. Distinctively, ORF3141 Δ sig protein was observed to
236 also induce cell apoptosis without targeting the mitochondria in FHM cells. Thus, it was proved that
237 the domain part without the signal peptide of ORF3141 protein had a critical relationship with cell
238 apoptosis whether it was targeted to the mitochondria or existent in the cytoplasm. Moreover,
239 quantitative assays of $\Delta\Psi_m$ value, caspase-3 activity, and apoptosis-related genes mRNA
240 expression were performed to determine how did the ORF3141 and ORF3141 Δ sig protein
241 participate in cell apoptosis in FHM cells. The Bcl-2 family proteins are critical regulators of
242 mitochondrial apoptosis, which include the anti-apoptotic multidomain members (containing all
243 four BH domains), the pro-apoptotic multidomain members (containing three BH domains), and
244 pro-apoptotic BH3-only members (containing the sole BH3 domain). In addition, a large number of

245 Bcl-2 family protein contain a hydrophobic transmembrane anchoring (TM) domain at the C-
246 terminus which allows them to co-localize to subcellular membranes [42,43]. Among these proteins,
247 Bcl-2 was discovered as an anti-apoptosis protein that blocks cell apoptosis, while Bax was clarified
248 as a pro-apoptosis protein which can form large openings in lipid bilayers to control the MOMP and
249 induce apoptosis [44–46]. Thus, a slight change in the dynamic balance of Bax and Bcl-2 seem to
250 determine the inhibition or promotion of cell apoptosis with apoptotic stimuli [47]. In fact, it is clear
251 that Bcl-2 family proteins can also localize to cytosol and other organelles, including the Golgi
252 apparatus, the endoplasmic reticulum (ER), and the nuclear out membrane (NOM) or the nucleus
253 itself [48]. In non-apoptotic cells, Bax localization is essentially diffuse in the cytosol but it is
254 relocated to mitochondria after cell apoptosis induction [49]. Therefore, it could be speculated that
255 both ORF3141 and ORF3141 Δ sig proteins were initiated by activating the apoptosis-related genes
256 (Bad, Bid, Bax, and Bcl-2) and induced the translocation of Bax from the cytosol to the
257 mitochondria in FHM cells. Besides, the relative ratio of *Bax* and *Bcl-2* genes mRNA expression
258 was out-of-balance, which were responsible for the $\Delta\Psi_m$ values declined and caspase-3 activity
259 increased in this study. Although the subcellular localization of ORF3141 and ORF3141 Δ sig
260 proteins were different, they could induce the cell apoptosis via the mitochondrial pathway.

261 Further studies are required to verify the mechanisms involved in ORF3141-induced cell
262 apoptosis by yeast two hybrid experiment. Whether the ORF3141 was the major virulence factor of
263 *N. seriolae* remains to be clarified by constructing Δ ORF3141 mutant attenuated and ORF3141
264 mutant completed *N. seriolae*. The relationship of the interaction between ORF3141 and
265 macrophage also need to be highlighted in future studies. In summary, we cloned an *ORF3141* gene
266 from *N. seriolae* strain ZJ0503 and analyzed its sequence structure. Moreover, MS analysis,
267 subcellular localization, overexpression assay, and apoptosis detection were performed. These
268 results showed that ORF3141 of *N. seriolae* strain ZJ0503 was a secreted protein that targeted the
269 host cell mitochondria and induced apoptosis in transfected FHM cells.

270

271

272

273 **Materials and methods**

274 **Bacterial strains, FHM cells, and plasmids**

275 *N. seriolae* strain ZJ0503 was isolated from diseased golden pompano (*T. ovatus*) in YangJiang
276 City, Guangdong Province, China [26] and was cultured in an optimized medium [glucose 20 g·L⁻¹,
277 yeast extract 15 g·L⁻¹, K₂HPO₄ 0.75 g·L⁻¹, CaCl₂ 0.2 g·L⁻¹ (sterilized separately), and NaCl 5 g·L⁻¹,
278 PH 6.5 ± 0.2)] at 28 °C [50]. *Escherichia coli* DH5α was used for gene cloning and it grown in
279 Luria-Bertani (LB) medium with vigorous shaking at 37 °C. Fathead minnow (FHM) epithelial cells
280 [51] were stored at -196 °C in Guangdong Provincial Key Laboratory of Pathogenic Biology and
281 Epidemiology for Aquatic Economic Animals and cultured at 25 °C in Leibovitz's L15 medium
282 containing 10% fetal bovine serum (Invitrogen, USA) in 5% CO₂ incubator. Plasmid pEGFP-N1
283 was used for subcellular localization, while pcDNA3.1/His A was used for overexpression.

284 **Ethics statement**

285 All animal experiments were handled in accordance with guidelines defined by the Institutional
286 Animal Care Use Committee (IACUC) of Guangdong Ocean University and were approved by
287 Guangdong Provincial Key Laboratory of Pathogenic Biology and Epidemiology for Aquatic
288 Economic Animals, following strict compliance with the regulations of the local government.

289 **Gene cloning and plasmid construction of *ORF3141* and *ORF3141*Δ*sig***

290 Genomic DNA was extracted from *N. seriolae* strain ZJ0503 using TIANamp Bacteria DNA Kit
291 (Tiangen, Beijing) following the manufacture's instruction. Four pairs of different primers were
292 carefully designed with corresponding restriction enzyme sites using Primer 5.0, on the basis of
293 *ORF3141* and *ORF3141*Δ*sig* genes of the whole genome sequence data of *N. seriolae* strain ZJ0503.
294 The PCR primers of pEGFP-3141F/R and pcDNA-3141F/R (Table 3) were used to amplify the
295 *ORF3141* gene. The PCR primers of pEGFP-3141Δ*sig*F/R and pcDNA-3141Δ*sig*F/R (Table 1)
296 were used to amplify the *ORF3141*Δ*sig* gene. The PCR procedures were performed with KOD-

297 plus-Neo DNA polymerase (Toyobo, Osaka, Japan), using the following PCR program: pre-
 298 denaturation at 98 °C for 2 min, 30 cycles at 98 °C for 10 s, 55 °C for 15 s, 69.5 °C for 15 s; and a
 299 final extension at 68 °C for 5 min. All PCR products of *ORF3141* and *ORF3141*Δsig genes were
 300 electrophoresed on 1% agarose gel and purified using EasyPure PCR Purification Kit (TRANSGEN,
 301 Beijing). The purified PCR product of *ORF3141* was digested by corresponding restriction enzymes,
 302 ligated into eukaryotic vectors pEGFP-N1 and pcDNA3.1/His A, respectively. And then
 303 transformed into competent *E. coli* DH5α cells. The different constructs were confirmed by
 304 corresponding restriction enzyme digestion and DNA sequencing by Guangzhou Sangon Biologic
 305 Engineering & Technology and Service Co. Ltd. The purified PCR product of *ORF3141*Δsig was
 306 processed similarly. Finally, the constructed recombinant plasmids were named as pEGFP-3141,
 307 pEGFP-3141Δsig, pcDNA-3141, and pcDNA-3141Δsig.

308

309

Table 1. Primers used for gene cloning

Gene Name	Primer Name	Sequence 5'-3'	Restriction endonucleases
ORF3141	pEGFP-3141F	GGAATTCATGAAGCTGCTGAACCCGCG	<i>Bam</i> H I
	pEGFP-3141R	CGGGATCCCGCTTGCCCGGGCAGGCGTTC	<i>Eco</i> R I
	pcDNA-3141F	CGGGATCCATGAAGCTGCTGAACCCGCG	<i>Eco</i> R I
	pcDNA-3141R	CGGAATTCCTTGCCCGGGCAGGCGTTCG	<i>Bam</i> H I
ORF3141Δsig	pEGFP-3141ΔsigF	GGAATTCATGGTCGAGGGTACCCCGACGGT C	<i>Eco</i> R I
	pEGFP-3141ΔsigR	CGGGATCCCGCTTGCCCGGGCAGGCGTTC	<i>Bam</i> H I
	pcDNA-3141ΔsigF	CGGGATCCATGGAGGGTACCCCGACGGT	<i>Bam</i> H I
	pcDNA-3141ΔsigR	CGGAATTCCTTGCCCGGGCAGGCGTTC	<i>Eco</i> R I

310 **Bioinformatics analysis, sequence alignments, and phylogenetic analysis**

311 Based on the whole genome sequence data of *N. seriolae* strain ZJ0503, sequence analysis was
 312 performed with the BLAST program using NCBI (<http://www.ncbi.nlm.nih.gov/BLAST/>). The
 313 amino acid sequence for ORF3141 was deduced, and the physical and chemical properties were

314 predicted using ExPASy software (<http://www.expasy.org/>). The location of domains was predicted
315 by the InterProScan program (<http://www.ebi.ac.uk/Tools/pfa/iprscan/>). The typical structures of
316 ORF3141 protein were predicted by I-TASSER online software
317 (<http://zhanglab.ccmb.med.umich.edu/I-TASSER/>). The potentially excreted proteins were
318 predicted by LocTree3 (<https://roslab.org/services/loctree/>) and ExPASy-PROSITE. The
319 subcellular localization and signal peptides were predicted with LocTree 3 and SignalP 4.1 Server
320 (www.cbs.dtu.dk/services/SignalP/), respectively. The MTSs were predicted using TarfetP
321 (<http://www.cbs.dtu.dk/services/TargetP/>) and PSORT II (<https://psort.hgc.jp/form2.html>). Protein
322 multiple sequence alignments of ORF3141 protein were performed by ClustalX 2.0 program with
323 the default parameters and edited by the GeneDoc software. The phylogenetic tree was generated
324 based on the deduced amino acid sequence of ORF3141 with the neighbor-joining method using
325 MEGA 6 program, in which the Poisson distribution substitution model and bootstrapping
326 procedure with 1000 bootstraps were applied.

327 **Preparation and identification of the *N. seriolae* extracellular products**

328 The extracellular products of *N. seriolae* strain ZJ0503 were obtained by cellophane overlay
329 method [52]. Specifically, *N. seriolae* were grown on optimized medium agar plate at 28 °C for 2 d,
330 and a single colony was prepared for bacterial suspension. Then, 100 µL of the bacterial suspension
331 was spread closely on optimized medium plates covered with sterile cellophane sheet and incubated
332 at 28 °C for 3 - 5 d. The *N. seriolae* cells grown on the cellophane sheet were stripped away from
333 the optimized medium plates, and the extracellular products were washed down with sterilized PBS
334 subsequently. The harvested suspension was centrifuged at 8000×g, 4 °C for 20 min, and the
335 supernatant containing extracellular products was filter sterilized with a 0.2 µm membrane filter.
336 Then, the sterilized supernatant was transferred into a dialysis tubing (3.5k MW) and dialyzed in
337 ultrapure water at 4 °C for 16 - 24 h. During dialysis, the ultrapure water was changed 3 - 4 times.
338 The purified supernatant was transferred into a centrifuge tube after dialysis and frozen under -80 °C.
339 Finally, it was lyophilized using a vacuum freeze dryer to obtain the protein dry powder which was
340 identified using shotgun MS.

341 **FHM cell mediated transient expression and subcellular localization**

342 Plasmids of pEGFP-3141, pEGFP-3141 Δ sig, and pEGFP-N1 were prepared in advance using
343 an endotoxin-free plasmid purification kit (Qiagen Inc., Chatsworth, CA). Subcellular localization
344 of ORF3141 and ORF3141 Δ sig proteins were performed through pEGFP-N1 fusion protein
345 expression. Given that a permanent FHM cell line is presently available, FHM cells were cultured
346 in 24-well plates and grown to 70 % confluency for transfection. The FHM cells were transfected
347 with empty pEGFP-N1 plasmids, recombinant pEGFP-3141 plasmids, and recombinant pEGFP-
348 3141 Δ sig plasmids using Lipofectamine 2000 (Invitrogen, Carlsbad, CA) according to the
349 manufacturer's protocol, respectively. At 48 hpt, the FHM cells were washed with PBS (pH 7.4),
350 stained with 300 nM MitoTracker Red CMXRos dye (Molecular Probes, Carlsbad, CA) at 28 °C for
351 45 min, fixed with 4% paraformaldehyde for 30 min, and labeled with 1 μ g/mL diamidino-2-
352 phenylindole (DAPI) at room temperature for 10 min. Finally, the cells were rinsed with PBS and
353 mounted with 50% glycerol. The fluorescence exhibited by the transfected FHM cells were
354 observed using a fluorescence microscope (Leica DM IRB).

355 **Overexpression of ORF3141 and ORF3141 Δ sig proteins in FHM cells**

356 The extraction and transfection of recombinant pcDNA-3141 plasmids, recombinant pcDNA-
357 3141 Δ sig plasmids, and control pcDNA3.1/His A plasmid were performed with reference to step
358 2.5. The transfected FHM cells were stained with DAPI at 48 hpt and microscopically observed to
359 test whether the overexpression of ORF3141 and ORF3141 Δ sig proteins induced apoptosis in fish
360 cells. Meanwhile, to identify the expression of ORF3141 and ORF3141 Δ sig proteins in the
361 transfected FHM cells, the cells were harvested at 48 hpt to extract the total RNA and proteins for
362 RT-PCR and Western blot analysis, respectively. RT-PCR was performed with primers pcDNA-
363 3141F/R and pcDNA-3141 Δ sigF/R (Table 3) following the synthesis of cDNA. Western blot was
364 conducted using mouse anti-His monoclonal antibody (Sigma, St. Louis, MO) as the primary
365 antibody at a dilution of 1:1000 and horseradish peroxidase-conjugated goat anti-mouse IgG (Sigma,
366 St. Louis, MO) as the secondary antibody at a dilution of 1:5000.

367 **Quantitative analysis of $\Delta\Psi_m$ value, caspase-3 activity and apoptosis-related gene**
368 **mRNA expression**

369 Several quantitative assays of mitochondrial membrane potential ($\Delta\Psi_m$) value, caspase-3 activity,
370 and apoptosis-related gene mRNA expression (pro-apoptotic gene: *Bad*, *Bid*, and *Bax*; anti-
371 apoptotic gene: *Bcl-2*), were performed to confirm the apoptosis caused by overexpression of
372 proteins in the transfected recombinant pcDNA-3141 or pcDNA3141 Δ sig in the FHM cells. The
373 $\Delta\Psi_m$ values were assessed at 24, 48, and 72 hpt using the JC-1 assay kit (Beyotime, Shanghai,
374 China) by the method described previously with minor modification [53]. The positive control was
375 treated with carbonyl cyanide 3-chlorophenylhydrazone (CCCP, 10 mM) to medium at 1:1000
376 25 °C for 20 min. Then, $\Delta\Psi_m$ value was measured by changes in the 590/530 JC-1 emitted
377 fluorescence with an Enspire 2300 Multilabel Reader (Perkin Elmer, MA, USA). The caspase-3
378 activity was detected in the FHM cells at 24 and 48 hpt as described previously [54] using a caspase-
379 3 colorimetric assay kit (BioVision, Milpitas, CA).

380 Three groups of transfected FHM cells were harvested at 0, 12, 24, 48, 60, and 72 hpt to extract
381 the total RNA, and quantitative real-time PCR (qRT-PCR) was performed following the synthesis
382 of cDNA. The cell apoptotic effect of post-transfection on the expression of apoptosis-related genes
383 mRNA, was investigated using real-time SYBR green PCR Master Mix on Applied Biosystems
384 7500 Real-Time PCR system (ABI, USA). Each assay was performed in triplicate with β -*actin* gene
385 as the internal control. According to the apoptosis gene sequence, five pairs of specific primer (Table
386 2) were carefully designed for qRT-PCR investigation. The PCR was performed in a 10 μ L reaction
387 volume containing 0.5 μ L of each primer (10 μ M), 0.3 μ L of cDNA, 3.7 μ L of PCR-grade water,
388 and 5 μ L of SYBR[®] Select Master Mix (ABI, USA) according to the manufacturer's protocol. The
389 PCR conditions were as follows: 95°C for 2 min; 40 cycles of 95 °C for 15 s, and 58 °C for 1 min
390 for four apoptosis-related genes and β -*actin*, respectively. Melt curve analysis of the amplification
391 products was performed over a range of 60 - 95 °C at the end of each PCR reaction to confirm the
392 single product generation. The relative expression levels of four apoptosis-related genes were
393 calculated using the comparative Ct $2^{(-\Delta\Delta C_t)}$ method [55].

394 **Table 2.** Primes used for apoptosis-related genes investigated by qRT-PCR.

Gene Name	Primer Name	Sequence 5'-3'
<i>β-actin</i>	β-actin-F	ACAATCAATACGGCTGCCATGG
	β-actin-R	TTGGCATAACAGGTCCTTACTTACGT
<i>Bad</i>	Bad-F	TGATCCTTTCAGGCGGAGATCTCGC
	Bad-R	CAGACTCTTTGTGACTCCAAAGGAA
<i>Bid</i>	Bid-F	CTGCTTCTCCTTTCCTTCTTTGAGC
	Bid-R	GATCAACTCAGCAGCCATATCCCTT
<i>Bax</i>	Bax-F	TGGCACTGTTTCACCTCG
	Bax-R	ATCCTCCTTGCTGTCTGATC
<i>Bcl-2</i>	Bcl-2-F	TGGGACTGTTTGCCTTCG
	Bcl-2-R	TCTGCCGCTGCATCTTTT

395

396 **Statistical analysis**

397 Data were presented as the means ± standard deviation (SD). Statistical analysis was performed
398 with one-way ANOVA with the SPSS statistics 21.0 software and the figures were edited by
399 GraphPad Prism software. Data represent the means for three independent experiments and
400 statistical significant is highlighted with asterisks in the figures as follows: $p > 0.05$, not significant;
401 $p < 0.05$ (*), significant; $p < 0.01$ (**), extremely significant. The means and p values for pairwise
402 comparisons of all experiments are provided in S3 Table.

403 **Acknowledgment**

404 We are grateful to all the laboratory members for the discussion and critical readings of the
405 manuscript.

406 **References**

407 1. Chen SC. Study on the pathogenicity of *Nocardia asteroides* to the Formosa snakehead, *Channa maculata*

- 408 (Lacepède), and largemouth bass, *Micropterus salmoides* (Lacepède). J Fish Dis. 2010;15: 47–53.
409 doi:10.1111/j.1365-2761.1992.tb00635.x
- 410 2. Pei-Chi W, Ming-An T, Yu-Chi L, Yanting C, Shih-Chu C. *Nocardia seriolae*, a causative agent of systematic
411 granuloma in spotted butterflyfish, *Scatophagus argus*, Linn. Afr J Microbiol Res. 2014;8: 3441–3452.
412 doi:10.5897/AJMR2014.6874
- 413 3. Xia L, Zhang H, Lu Y, Cai J, Wang B, Jian J. Development of a Loop-Mediated Isothermal Amplification
414 Assay for Rapid Detection of *Nocardia salmonicida*, the Causative Agent of Nocardiosis in Fish. J Microbiol
415 Biotechnol. 2015;25: 321–327. doi:10.4014/jmb.1406.06052
- 416 4. Vu-Khac H, Duong VQB, Chen S-C, Pham TH, Nguyen TTG, Trinh TTH. Isolation and genetic
417 characterization of *Nocardia seriolae* from snubnose pompano *Trachinotus blochii* in Vietnam. Dis Aquat
418 Organ. 2016;120: 173–177. doi:10.3354/dao03023
- 419 5. Ho PY, Byadgi O, Wang PC, Tsai MA, Liaw LL, Chen SC. Identification, Molecular Cloning of IL-1 β and
420 Its Expression Profile during *Nocardia seriolae* Infection in Largemouth Bass, *Micropterus salmoides*: Int J
421 Mol Sci. 2016;17. doi:10.3390/ijms17101670
- 422 6. Labrie L, Ng J, Tan Z, Komar C, Ho E, Grisez L, et al. Nocardial infections in fish: an emerging problem in
423 both freshwater and marine aquaculture systems in Asia. Dis Asian Aquac VI. 2005;
- 424 7. Elkesh A, Kantham KPL, Shinn AP, Crumlish M, Richards RH. Systemic nocardiosis in a Mediterranean
425 population of cultured meagre, *Argyrosomus regius* Asso (Perciformes: Sciaenidae). J Fish Dis. 2013;36:
426 141–149. doi:10.1111/jfd.12015
- 427 8. Manrique WG, Da SCG, de Castro MP, Petrillo TR, Figueiredo MA, Ma DAB, et al. Expression of Cellular
428 Components in Granulomatous Inflammatory Response in *Piaractus mesopotamicus* Model. Plos One.
429 2015;10: e0121625.
- 430 9. Maekawa S, Yoshida T, Wang P-C, Chen S-C. Current knowledge of nocardiosis in teleost fish. J Fish Dis.
431 2018;41: 413–419. doi:10.1111/jfd.12782
- 432 10. Wang GL, Yuan SP, Jin S. Nocardiosis in large yellow croaker, *Larimichthys crocea* (Richardson). J Fish
433 Dis. 2005;28: 339–345. doi:10.1111/j.1365-2761.2005.00637.x
- 434 11. Wang GL, Yi-Jun XU, Jin S. Identification and phylogenetic analyses of *Nocardia* in snakehead,
435 *Ophiocephalus argus* Cantor. J Fish China. 2008;32: 449–454.
- 436 12. Beaman BL, Beaman L. *Nocardia* species: host-parasite relationships. Clin Microbiol Rev. 1994;7: 213–64.
- 437 13. Barry DP, Beaman BL. *Nocardia asteroides* strain GUH-2 induces proteasome inhibition and apoptotic death
438 of cultured cells. Res Microbiol. 2007;158: 86–96. doi:10.1016/j.resmic.2006.11.001
- 439 14. Camp DM, Loeffler DA, Razoky BA, Tam S, Beaman BL, LeWitt PA. *Nocardia asteroides* culture filtrates
440 cause dopamine depletion and cytotoxicity in PC12 cells. Neurochem Res. 2003;28: 1359–1367.
441 doi:10.1023/A:1024944431725

- 442 15. Loeffler DA, Camp DM, Qu S, Beaman BL, LeWitt PA. Characterization of dopamine-depleting activity of
443 *Nocardia asteroides* strain GUH-2 culture filtrate on PC12 cells. *Microb Pathog.* 2004;37: 73–85.
444 doi:10.1016/j.micpath.2004.05.001
- 445 16. Lartigue L, Faustin B. Mitochondria: Metabolic regulators of innate immune responses to pathogens and cell
446 stress. *Int J Biochem Cell Biol.* 2013;45: 2052–2056. doi:10.1016/j.biocel.2013.06.014
- 447 17. Rudel T, Kepp O, Kozjak-Pavlovic V. Interactions between bacterial pathogens and mitochondrial cell death
448 pathways. *Nat Rev Microbiol.* 2010;8: 693–705. doi:10.1038/nrmicro2421
- 449 18. Saint-Georges-Chaumet Y, Edeas M. Microbiota-mitochondria inter-talk: consequence for microbiota-host
450 interaction. *Pathog Dis.* 2016;74: ftv096. doi:10.1093/femspd/ftv096
- 451 19. West AP, Shadel GS, Ghosh S. Mitochondria in innate immune responses. *Nat Rev Immunol.* 2011;11: 389–
452 402. doi:10.1038/nri2975
- 453 20. Rudel T, Kepp O, Kozjak-Pavlovic V. Interactions between bacterial pathogens and mitochondrial cell death
454 pathways. *Nat Rev Microbiol.* 2010;8: 693–705. doi:10.1038/nrmicro2421
- 455 21. Neely AM, Zhao G, Schwarzer C, Stivers NS, Whitt AG, Meng S, et al. N-(3-Oxo-acyl)-homoserine lactone
456 induces apoptosis primarily through a mitochondrial pathway in fibroblasts. *Cell Microbiol.* 2018;20: e12787.
457 doi:10.1111/cmi.12787
- 458 22. Karijolich J, Abernathy E, Glaunsinger BA. Infection-Induced Retrotransposon-Derived Noncoding RNAs
459 Enhance Herpesviral Gene Expression via the NF-kappa B Pathway. *Plos Pathogens.* 2015;11: e1005260.
460 doi:10.1371/journal.ppat.1005260
- 461 23. Chen AW-G, Tseng Y-S, Lin C-C, Hsi Y-T, Lo Y-S, Chuang Y-C, et al. Norcantharidin induce apoptosis in
462 human nasopharyngeal carcinoma through caspase and mitochondrial pathway. *Environ Toxicol.* 2018;33:
463 343–350. doi:10.1002/tox.22521
- 464 24. Huang T-C, Chiu P-R, Chang W-T, Hsieh B-S, Huang Y-C, Cheng H-L, et al. Epirubicin induces apoptosis
465 in osteoblasts through death-receptor and mitochondrial pathways. *Apoptosis.* 2018;23: 226–236.
466 doi:10.1007/s10495-018-1450-2
- 467 25. Tang C, Wang J, Wei Q, Du Y-P, Qiu H-P, Yang C, et al. Tropomyosin-1 promotes cancer cell apoptosis via
468 the p53-mediated mitochondrial pathway in renal cell carcinoma. *Oncol Lett.* 2018;15: 7060–7068.
469 doi:10.3892/ol.2018.8204
- 470 26. Xia L, Cai J, Wang B, Huang Y, Jian J, Lu Y. Draft Genome Sequence of *Nocardia seriolae* ZJ0503, a Fish
471 Pathogen Isolated from *Trachinotus ovatus* in China. *Genome Announc.* 2015;3:
472 doi:10.1128/genomeA.01223-14
- 473 27. Dawson RJ, Locher KP. Structure of the multidrug ABC transporter Sav1866 from *Staphylococcus aureus* in
474 complex with AMP-PNP. *Febs Lett.* 2007;581: 935. doi:10.1016/j.febslet.2007.01.073
- 475 28. Imajoh M, Fukumoto Y, Jin Y, Sukeda M, Shimizu M, Ohnishi K, et al. Draft Genome Sequence of *Nocardia*

- 476 *seriolae* Strain N-2927 (NBRC 110360), Isolated as the Causal Agent of Nocardiosis of Yellowtail (*Seriola*
477 *quinqueradiata*) in Kochi Prefecture, Japan. *Genome Announc.* 2015;3: e00082-15.
- 478 29. Imajoh M, Sukeda M, Shimizu M, Yamane J, Ohnishi K, Oshima S. Draft Genome Sequence of
479 Erythromycin- and Oxytetracycline-Sensitive *Nocardia seriolae* Strain U-1 (NBRC 110359). *Genome*
480 *Announc.* 2016;4: e01606-15.
- 481 30. Yasuike M, Nishiki I, Iwasaki Y, Nakamura Y, Fujiwara A, Shimahara Y, et al. Analysis of the complete
482 genome sequence of *Nocardia seriolae* UTF1, the causative agent of fish nocardiosis: The first reference
483 genome sequence of the fish pathogenic *Nocardia* species. *Plos One.* 2017;12: e0173198.
484 doi:10.1371/journal.pone.0173198
- 485 31. Cai J, Huang Y, Wei S, Ouyang Z, Huang X, Qin Q. Characterization of LPS-induced TNF α factor (LITAF)
486 from orange-spotted grouper, *Epinephelus coioides*. *Fish and Shellfish Immunol.* 2013;35: 1858–1866.
487 doi:10.1016/j.fsi.2013.09.023
- 488 32. Chen H, Niu X, Gao A, Zhang S. Mitochondrial signal peptide guides EGFP-GRP75 fusion proteins into
489 mitochondria. *Xi Bao Yu Fen Zi Mian Yi Xue Za Zhi Chin J Cell Mol Immunol.* 2016;32: 1311–1316.
- 490 33. Habib SJ, Neupert W, Rapaport D. Analysis and prediction of mitochondrial targeting signals. In: Pon LA,
491 Schon EA, editors. *Mitochondria*, 2nd Edition. San Diego: Elsevier Academic Press Inc; 2007. pp. 761–781.
- 492 34. Habib SJ, Neupert W, Rapaport D. Analysis and prediction of mitochondrial targeting signals. *Methods Cell*
493 *Biol.* 2007;80: 761–781.
- 494 35. Bohni PC, Daum G, Schatz G. Import of proteins into mitochondria. Partial purification of a matrix-located
495 protease involved in cleavage of mitochondrial precursor polypeptides. *J Biol Chem.* 1983;258: 4937–43.
- 496 36. Hawlitschek G, Schneider H, Schmidt B, Tropschug M, Hartl FU, Neupert W. Mitochondrial protein import:
497 identification of processing peptidase and of PEP, a processing enhancing protein. *Cell.* 1988;53: 795–806.
498 doi:10.1016/0092-8674(88)90096-7
- 499 37. Nagai T, Abe A, Sasakawa C. Targeting of enteropathogenic *Escherichia coli* EspF to host mitochondria is
500 essential for bacterial pathogenesis - Critical role of the 16th leucine residue in EspF. *J Biol Chem.* 2005;280:
501 2998–3011. doi:10.1074/jbc.M411550200
- 502 38. Ma C, Wickham ME, Guttman JA, Deng W, Walker J, Madsen KL, et al. *Citrobacter rodentium* infection
503 causes both mitochondrial dysfunction and intestinal epithelial barrier disruption in vivo: role of
504 mitochondrial associated protein (Map). *Cell Microbiol.* 2006;8: 1669–1686. doi:10.1111/j.1462-
505 5822.2006.00741.x
- 506 39. Choi CH, Lee EY, Lee YC, Park TI, Kim HJ, Hyun SH, et al. Outer membrane protein 38 of *Acinetobacter*
507 *baumannii* localizes to the mitochondria and induces apoptosis of epithelial cells. *Cell Microbiol.* 2005;7:
508 1127–1138. doi:10.1111/j.1462-5822.2005.00538.x
- 509 40. Muller A, Rassow J, Grimm J, Machuy N, Meyer TF, Rudel T. VDAC and the bacterial porin PorB of
510 *Neisseria gonorrhoeae* share mitochondrial import pathways. *Embo J.* 2002;21: 1916–1929.

- 511 doi:10.1093/emboj/21.8.1916
- 512 41. Hernandez LD, Pypaert M, Flavell RA, Galan JE. A Salmonella protein causes macrophage cell death by
513 inducing autophagy. *J Cell Biol.* 2003;163: 1123–1131. doi:10.1083/jcb.200309161
- 514 42. Ola MS, Nawaz M, Ahsan H. Role of Bcl-2 family proteins and caspases in the regulation of apoptosis. *Mol*
515 *Cell Biochem.* 2011;351: 41–58. doi:10.1007/s11010-010-0709-x
- 516 43. Edlich F. BCL-2 proteins and apoptosis: Recent insights and unknowns. *Biochem Biophys Res Commun.*
517 2018;500: 26–34. doi:10.1016/j.bbrc.2017.06.190
- 518 44. Pan Y, Ye C, Tian Q, Yan S, Zeng X, Xiao C, et al. miR-145 suppresses the proliferation, invasion and
519 migration of NSCLC cells by regulating the BAX/BCL-2 ratio and the caspase-3 cascade. *Oncol Lett.*
520 2018;15: 4337–4343. doi:10.3892/ol.2018.7863
- 521 45. Kalkavan H, Green DR. MOMP, cell suicide as a BCL-2 family business. *Cell Death Differ.* 2018;25: 46–
522 55. doi:10.1038/cdd.2017.179
- 523 46. Shimizu S, Narita M, Tsujimoto Y. Bcl-2 family proteins regulate the release of apoptogenic cytochrome c
524 by the mitochondrial channel VDAC. *Nature.* 1999;399: 483–487. doi:10.1038/20959
- 525 47. Liu JJ, Huang RW, Lin DJ, Peng J, Wu XY, Lin Q, et al. Expression of survivin and bax/bcl-2 in peroxisome
526 proliferator activated receptor-gamma ligands induces apoptosis on human myeloid leukemia cells in vitro.
527 *Ann Oncol.* 2005;16: 455–459. doi:10.1093/annonc/mdi077
- 528 48. Popgeorgiev N, Jabbour L, Gillet G. Subcellular Localization and Dynamics of the Bcl-2 Family of Proteins.
529 *Front Cell Dev Biol.* 2018;6: 13. doi:10.3389/fcell.2018.00013
- 530 49. Wolter KG, Hsu YT, Smith CL, Nechushtan A, Xi XG, Youle RJ. Movement of Bax from the cytosol to
531 mitochondria during apoptosis. *J Cell Biol.* 1997;139: 1281–92.
- 532 50. Xia L, Wang B, Xia H, Huang Y, Jian J, Yishan LU. Optimal culture conditions and medium of *Nocardia*
533 *serioleae*. *South China Fish Sci.* 2013;9: 51–56.
- 534 51. Gravell M, Malsberger RG. A permanent cell line from the fathead minnow (*Pimephales promelas*). *Ann N*
535 *Y Acad Sci.* 1965;126: 555–65. doi:10.1111/j.1749-6632.1965.tb14302.x
- 536 52. Xia L, Liang H, Xu L, Chen J, Bekaert M, Zhang H, et al. Subcellular localization and function study of a
537 secreted phospholipase C from *Nocardia serioleae*. *FEMS Microbiol Lett.* 2017;364.
538 doi:10.1093/femsle/fnx143
- 539 53. Sun YS, Lv LX, Zhao Z, He X, You L, Liu JK, et al. Cordycepol C induces caspase-independent apoptosis
540 in human hepatocellular carcinoma HepG2 cells. *Biol Pharm Bull.* 2014;37: 608–17.
- 541 54. Zhao Z, Chen C, Hu C-Q, Ren C-H, Zhao J-J, Zhang L-P, et al. The type III secretion system of *Vibrio*
542 *alginolyticus* induces rapid apoptosis, cell rounding and osmotic lysis of fish cells. *Microbiol-Sgm.* 2010;156:
543 2864–2872. doi:10.1099/mic.0.040626-0

544 55. Yang X. Analysis of the copy number of exogenous genes in transgenic cotton using real-time quantitative
545 PCR and the 2- $\Delta\Delta$ CT method. Afr J Biotechnol. 2012;11. doi:10.5897/AJB11.4117

546

547 **Supporting information**

548 **S1 Table.** Compared with the homology of ORF3141 among other *Nocardia* species.

549 **S2 Table.** The same sequence of ORF3141 between different *N. seriolae* strain.

550 **S3 Table.** Statistical analysis of all experimental data.

551 **Figure captions**

552 **Fig 1. Sequence and structure analysis of ORF3141 from *N. seriolae*.** (A) The full lengths
553 nucleotide and deduced amino acid sequence of *ORF3141* gene. The underline amino acid sequence
554 showed the signal peptide. (B) Schematic representation of the domain topology of ORF3141. The
555 ORF3141 protein was comprised of a signal peptide at N-terminate (residues 1-30), two low
556 complexity domains (residues 47-70, 90-117), and five kinds of functional sites. (C) The three-
557 dimensional structures of ORF3141 protein from *N. seriolae* (Left) and the closest structure to
558 multidrug ABC transporter Sav1866 from *Staphylococcus aureus* (Right). The diagrams were
559 generated using I-TASSER online and PyMOL 1.8 software.

560

561 **Fig 2. Multiple sequence alignment and construction of phylogenetic tree.** (A) Multiple
562 alignment of the deduced amino acid sequences of ORF3141 protein among different species.
563 Shaded regions indicate residues sharing homology, black regions indicate 100 % homology, dark
564 gray regions indicate homology higher than 75 %. (B) Construction of phylogenetic tree among *N.*
565 *seriolae* and other species with ORF3141 protein homology sequences. Protein sequences were
566 aligned with Clustal W, and the nonrooted neighbor-joining tree was generated by MEGA 5.0
567 program. Number at branch points indicate bootstrap support. GenBank accession numbers are
568 shown as followed: *Mycobacterium tuberculosis* H37Ra (ABQ74022.1), *Mycobacterium marinum*
569 M (ACC41759.1), *Mycobacterium rhodesiae* NBB3 (AEV74934.1), *Skermania piniformis*

570 (WP_066468955.1), *Gordonia soli* NBRC 108243 (GAC69437.1), *Gordonia polyisoprenivorans*
571 NBRC 16320 (GAB24816.1), *Gordonia alkanivorans* NBRC 16433 (GAA10605.1), *Rhodococcus*
572 *globorulus* (WP_045067034.1), *Rhodococcus opacus* (WP_012688156.1), *Rhodococcus koreensis*
573 (WP_072945555.1), *Nocardia seriolae* ZJ0503 (WP_033086993.1), *Nocardia concave*
574 (WP_040804030.1), *Nocardia pneumonia* (WP_040776180.1), *Nocardia brasiliensis* NBRC 14402
575 (GAJ80338.1), *Streptomyces ochraceiscleroticus* (WP_031055338.1), *Streptomyces violens*
576 (WP_030248901.1).

577

578 **Fig 3. Subcellular localization of ORF3141 and ORF3141 Δ sig proteins in FHM cell.** Green
579 fluorescence shows the ORF3141-GFP, ORF3141 Δ sig-GFP or GFP, red fluorescence shows the
580 mitochondria, blue fluorescence shows the nucleus, and the arrow refers to the nuclear
581 fragmentation and condensation. In the control plasmid pEGFP-N1, the green fluorescence was
582 evenly distributed in the whole cell of FHM cells, mitochondria were annularly distributed in the
583 periphery of nucleus, the edge of nucleus was smooth with uniform dyeing and had no apoptosis
584 characteristics. Subcellular localization of ORF3141-GFP fusion proteins were mainly distributed
585 in the cytoplasm that coincided with the distribution of mitochondria, which indicated that the
586 protein ORF3141 is targeted to mitochondria. Differently, subcellular localization of
587 ORF3141 Δ sig-GFP fusion proteins were evenly distributed in the whole cell of FHM cells, and
588 were not coincide with the distribution of mitochondria, which indicated that the subcellular
589 localization changed with the excision of signal peptide. The expression of ORF3141 or
590 ORF3141 Δ sig proteins changed the distribution of mitochondria from perinuclear halo into lumps
591 and apoptotic bodies were detected.

592

593 **Fig 4. Overexpression of ORF3141 and ORF3141 Δ sig proteins in FHM cells.** The transfected
594 cells were fixed at 48 h post-transfection staining by DAPI. Arrows indicated the apoptotic bodies
595 (fragmented nucleus), arrow heads indicated the apoptotic cells.

596

597 **Fig 5. Apoptosis nucleus ratio, RT-PCT, and Western blot of pcDNA-3141 and pcDNA-**
598 **3141 Δ sig transfected FHM cells.** (A) The apoptotic nucleus was counted and the percentages of

599 apoptotic cells were calculated. Data represent the means for three independent experiments and
600 error bars indicate SD (** $p < 0.01$). (B) Confirmation of the ORF3141 and ORF3141 Δ sig
601 expression in FHM cells by RT-PCR. Lane M, DNA marker; lane 1, pcDNA-3141 Δ sig/FHM; lane
602 2, pcDNA-3141/FHM. (C) Confirmation of the ORF3141 expression in FHM cells by western blot.
603 Lane M, Protein marker; lane 1, pcDNA-3141/FHM; lane 2, pcDNA 3.1 His/A (Up) and
604 confirmation of the ORF3141 Δ sig expression in FHM cells by western blot. Lane M, protein marker;
605 lane 1, pcDNA 3.1 His/A; lane 2, pcDNA-3141 Δ sig/FHM (Down).

606

607 **Fig 6. Apoptotic detection of ORF3141 and ORF3141 Δ sig overexpressed FHM cells.** (A)

608 Mitochondrial membrane potential assay. FHM cells transfected with pcDNA-3141, pcDNA-
609 3141 Δ sig or pcDNA 3.1 His/A plasmid were collected at indicated time points after transfection
610 and the mitochondrial membrane potential were assessed using the JC-1. Un-transfected cells
611 treated with CCCP was positive control. The data were expressed as the JC-1 polymer/monomer
612 fluorescence ratio and error bars indicate SD (* $p < 0.05$, ** $p < 0.01$). (B) Measurement of caspase-3
613 activity. FHM cells transfected with pcDNA-3141, pcDNA-3141 Δ sig or pcDNA 3.1 His/A plasmid
614 were collected at indicated time points after transfection and the levels of cleaved caspase-3 were
615 measured. The data were expressed as fold increase compared to the corresponding caspase-3
616 activity values in un-transfected cells and error bars indicate SD (* $p < 0.05$, ** $p < 0.01$). (C) qRT-
617 PCR analysis of the expression of apoptosis-related genes (*Bad*, *Bid*, *Bax*, and *Bcl-2*) and error bars
618 indicate SD (* $p < 0.05$, ** $p < 0.01$).

619

620

A

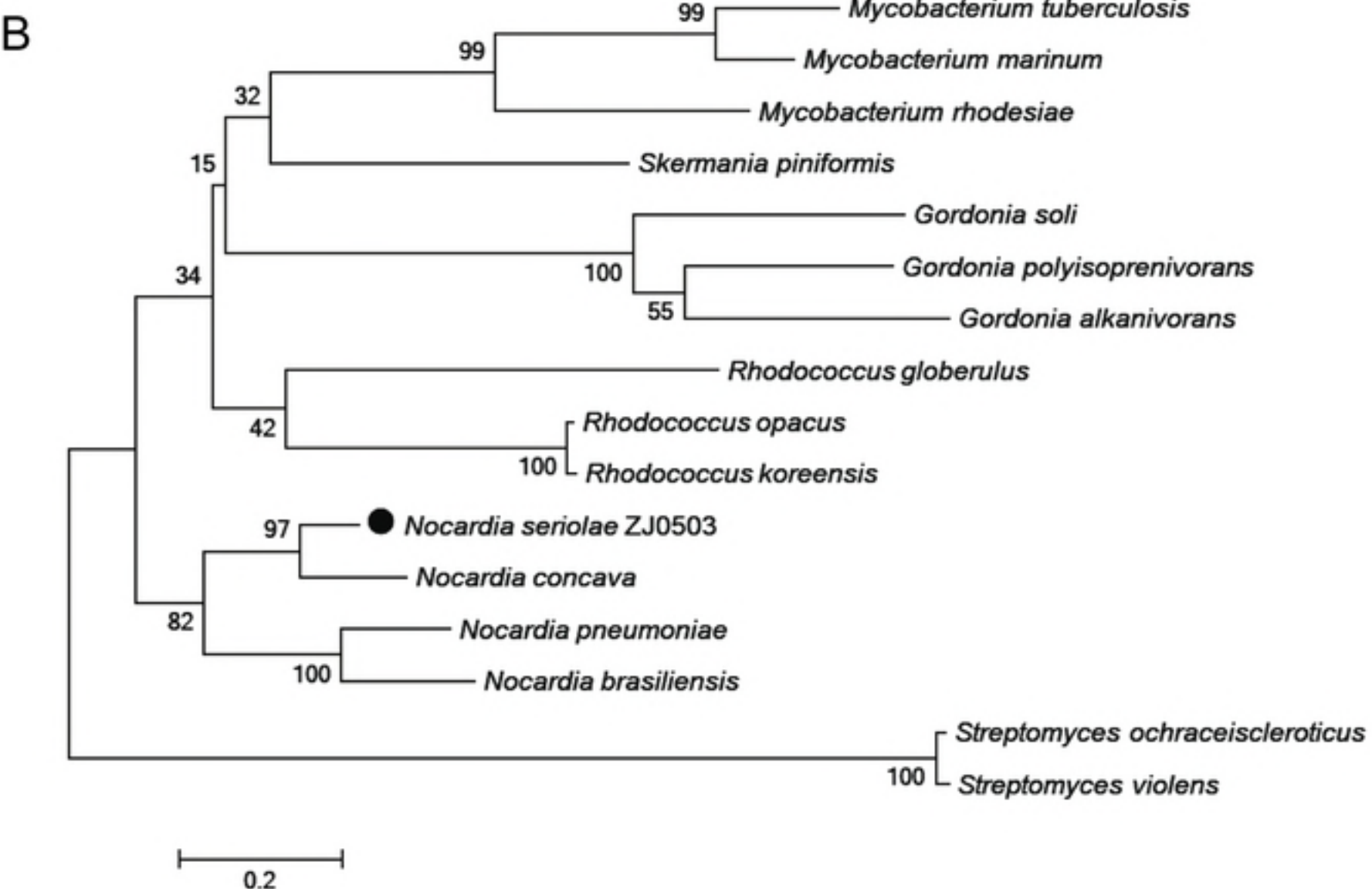
N. seriolae : -----M~~LLN~~-----P~~RGF~~L~~V~~C-----A~~SAA~~V~~AAG~~ : 21
N. concava : -----M~~LLN~~-----P~~RGF~~L~~V~~C-----A~~SAA~~V~~AAG~~ : 21
N. brasiliensis : -----M~~RTLD~~-----P~~RRF~~L~~I~~C-----A~~TGA~~V~~AVG~~ : 21
M. rhodesia : -----M~~V~~T~~G~~W-L~~C~~P~~R~~-----R~~L~~R~~F~~A~~A~~L-----V~~V~~G~~S~~I~~A~~A~~S~~ : 24
M. marinum : -----M~~L~~I~~G~~W~~R~~A~~V~~P~~R~~R~~H~~G~~G~~A~~F~~S~~G~~S~~R~~A~~R~~R~~G~~A~~Q~~-----A~~L~~G~~C~~I~~A~~V~~L~~ : 34
S. piniformis : -----M~~R~~T~~E~~Q~~R~~-----Y~~R~~R~~A~~L~~T~~G-----A~~M~~T~~A~~A~~I~~T~~M~~ : 22
R. globerulus : -----M~~K~~A~~G~~P~~V~~R~~G~~S~~G~~K~~S~~V~~D~~R~~Y~~R~~R~~R~~L~~V~~V~~-----A~~I~~G~~A~~I~~T~~V~~G~~ : 31
R. opacus : -----M~~R~~T~~S~~S-----R~~R~~W~~L~~L~~S~~-----A~~A~~A~~A~~A~~I~~V~~G~~ : 20
G. polyisoprenivorans : M~~R~~R~~A~~S~~A~~R~~R~~A~~R~~A~~R~~A~~E~~L~~R~~N~~V~~G~~G~~C~~H~~S~~G~~T~~E~~E~~C~~H~~Q~~T~~D~~A~~D~~Q~~R~~S~~G~~V~~L~~R~~V~~R~~R~~T~~A~~G~~A~~T~~R~~V~~G~~V~~T~~V~~L~~T~~A~~V~~I~~T~~A~~A : 66
G. soli : -----M~~Q~~L~~G~~D~~C~~A~~L~~-----A~~R~~D~~T~~A~~P~~V~~G~~G~~R~~G-----A~~V~~S~~R~~R~~R~~G~~C~~-----V~~A~~L~~A~~I~~V~~A~~G~~ : 34

N. seriolae : -----L~~M~~I~~A~~G~~G~~A~~N~~T~~V~~E~~G~~I~~P~~T~~V~~I~~Q~~A~~Q~~V~~T~~S~~S~~Y~~R~~A~~E~~V~~S~~S~~S~~A~~A~~A~~S~~S~~S~~K~~A~~A~~A~~A~~Q~~-----V~~A~~K~~I~~T~~A~~D~~N~~C~~D~~ : 74
N. concava : -----L~~V~~L~~A~~G~~G~~S~~N~~T~~V~~E~~G~~I~~P~~T~~V~~I~~Q~~A~~E~~V~~T~~S~~S~~Y~~K~~A~~A~~A~~A~~T~~S~~A~~A~~A~~S~~S~~A~~K~~A~~A~~A~~A-----V~~A~~K~~I~~T~~A~~D~~N~~C~~D~~ : 74
N. brasiliensis : -----L~~V~~V~~A~~G~~G~~G~~N~~R~~V~~H~~G~~I~~P~~N~~P~~N~~T~~A~~D~~L~~A~~A~~Y~~K~~T~~E~~A~~A~~A~~S~~S~~A~~A~~A~~T~~S~~S~~K~~R~~A~~A~~A-----Q~~T~~K~~I~~G~~D~~N~~C~~A : 74
M. rhodesia : -----A~~M~~I~~V~~V~~G~~G~~S~~N~~V~~T~~E~~C~~K~~P~~S~~V~~I~~S~~A~~D~~A~~P~~V~~Y~~R~~A~~S~~V~~S~~A~~S~~I~~Q~~E~~S~~I~~A~~S~~S~~S~~A~~R~~E~~S~~E~~R~~Q~~E~~S~~L~~T~~Q~~E~~V~~H~~T~~S~~C~~E~~ : 85
M. marinum : -----L~~M~~G~~I~~V~~G~~C~~T~~S~~V~~T~~D~~G~~I~~A~~T~~P~~D~~T~~K~~V~~A~~P~~A~~Y~~R~~S~~S~~V~~S~~M~~S~~I~~S~~I~~S~~A~~A~~T~~S~~S~~V~~R~~E~~S~~Q~~R~~Q~~S~~L~~T~~T~~K~~I~~R~~T~~S~~C~~E : 95
S. piniformis : T~~V~~A~~V~~I~~A~~I~~V~~V~~A~~G~~G~~D~~R~~I~~D~~G~~S~~A~~R~~E~~N~~S~~G~~E~~A~~S~~A~~Y~~R~~S~~E~~A~~A~~A~~S~~S~~S~~A~~A~~A~~A~~A~~Q~~A~~A~~A-----T~~A~~K~~I~~K~~A~~D~~T~~C~~G~~ : 81
R. globerulus : -----S~~V~~V~~I~~V~~G~~C~~S~~G~~A~~V~~E~~C~~S~~P~~T~~P~~N~~R~~V~~Q~~A~~A~~A~~Y~~Q~~A~~E~~V~~T~~A~~S~~-I~~A~~S~~S~~S~~K~~A~~A~~A~~D~~-----A~~V~~E~~T~~A~~F~~Q~~T~~C~~E~~ : 84
R. opacus : -----A~~G~~V~~I~~A~~G~~G~~G~~A~~T~~E~~G~~I~~A~~Q~~Q~~N~~D~~S~~Q~~A~~E~~Y~~A~~A~~E~~A~~T~~S~~S~~V~~A~~S~~S~~S~~Q~~K~~A~~A~~D~~-----E~~R~~E~~L~~V~~E~~Q~~O~~T : 74
G. polyisoprenivorans : -----V~~L~~I~~F~~A~~G~~C~~A~~T~~S~~I~~P~~C~~A~~P~~T~~V~~I~~S~~A~~Q~~V~~S~~M~~Y~~R~~S~~E~~Q~~S~~A~~S~~T~~S~~A~~R~~R-----E~~L~~A~~V~~T~~L~~O~~R~~ : 112
G. soli : -----A~~V~~I~~V~~G~~G~~C~~S~~-S~~V~~D~~G~~S~~G~~T~~A~~A~~S~~G~~V~~A~~A~~Y~~R~~A~~E~~V~~T~~A~~S~~R~~A~~E~~V~~Q-----K~~A~~G~~T~~D~~V~~C~~S~~ : 79

bioRxiv preprint doi: <https://doi.org/10.1101/341651>; this version posted June 7, 2018. The copyright holder for this preprint (which was not certified by peer review) is the author/funder, who has granted bioRxiv a license to display the preprint in perpetuity. It is made available under aCC-BY 4.0 International license.

N. seriolae : P~~R~~R~~K~~I~~A~~G~~T~~A~~V~~N~~V~~V~~A~~F~~V~~D~~A~~H~~L~~C~~A~~S~~A~~A~~D~~Q~~L~~T~~K~~R~~D~~A~~A~~T~~A~~L~~E~~D~~A~~K~~G~~V~~E~~T~~Q~~L~~T~~A~~T~~G~~A~~A~~P~~A~~D~~I~~A~~G~~K~~L~~T~~D : 140
N. concava : P~~F~~R~~K~~S~~A~~G~~N~~A~~V~~D~~R~~I~~N~~E~~F~~V~~D~~A~~H~~L~~C~~A~~S~~A~~A~~D~~Q~~L~~T~~K~~R~~D~~A~~A~~T~~A~~L~~E~~D~~A~~K~~G~~V~~E~~T~~Q~~L~~T~~A~~T~~G~~A~~A~~P~~A~~D~~I~~A~~G~~K~~F~~T~~D~~ : 140
N. brasiliensis : Q~~F~~P~~T~~T~~T~~G~~V~~G~~V~~S~~K~~Y~~N~~E~~F~~I~~D~~A~~H~~L~~C~~A~~N~~A~~G~~D~~Y~~A~~A~~K~~R~~E~~L~~A~~S~~T~~L~~D~~D~~A~~N~~K~~V~~E~~T~~G~~I~~S~~T~~A~~K~~D~~A~~P~~A~~D~~I~~A~~A~~K~~F~~T~~D~~ : 140
M. rhodesia : S~~L~~S~~T~~S~~S~~V~~D~~A~~I~~T~~A~~V~~N~~A~~Y~~V~~D~~A~~F~~N~~Q~~S~~A~~A~~D~~A~~E~~A~~K~~A~~G~~P~~I~~D~~A~~L~~N~~H~~S~~A~~D~~L~~V~~G---G~~S~~V~~S~~D~~P~~I~~T~~P~~E~~I~~K~~D~~A~~M~~R~~S : 148
M. marinum : T~~L~~A~~T~~T~~S~~S~~K~~E~~A~~I~~D~~K~~V~~N~~E~~F~~V~~G~~A~~F~~N~~-A~~G~~R~~S~~T~~G~~P~~T~~E~~G~~P~~I~~E~~A~~L~~N~~N~~S~~I~~S~~S~~V~~S---S~~A~~L~~N~~E~~A~~I~~S~~P~~D~~I~~R~~D~~A~~F~~N~~A : 157
S. piniformis : A~~F~~L~~G~~R~~T~~D~~P~~A~~I~~D~~A~~F~~N~~G~~F~~V~~D~~A~~S~~N~~K~~R~~A~~D~~D~~I~~A~~A~~R~~R~~S~~A~~V~~T~~E~~L~~R~~K~~S~~I~~D~~E~~V~~D~~A~~G~~V~~Q~~A~~A~~G~~P~~P~~I~~D~~P~~I~~A~~K~~R~~F~~A~~D~~ : 147
R. globerulus : E~~L~~I~~R~~R~~S~~K~~D~~D~~V~~A~~V~~F~~N~~A~~Y~~I~~D~~A~~N~~N~~D~~E~~S~~D~~V~~T~~S~~K~~A~~Q~~A~~A~~S~~A~~S~~A~~D~~E~~F~~I~~G~~----W~~L~~D~~T~~A~~T~~A~~D~~V~~P~~A~~S~~I~~S~~G~~L~~F~~G~~D : 146
R. opacus : M~~F~~V~~T~~R~~A~~G~~E~~T~~I~~D~~T~~Y~~N~~T~~F~~I~~D~~A~~A~~N~~A~~E~~A~~A~~D~~T~~G~~A~~K~~A~~S~~A~~A~~A~~L~~R~~S~~A~~D~~---G~~A~~N~~A~~A~~T~~P~~A~~I~~P~~P~~D~~I~~T~~G~~L~~L~~T~~D : 136
G. polyisoprenivorans : Q~~A~~M~~S~~S~~M~~V~~V~~M~~V~~R~~G~~I~~N~~T~~F~~V~~R~~L~~N~~-A~~V~~Q~~S~~Y~~D~~R~~V~~G~~D~~L~~D~~D~~R~~A~~R~~A~~S~~L~~I~~A~~G~~V~~D~~Q~~I~~R~~A~~K~~V~~T~~G~~A~~V~~T~~A~~D~~V~~T~~G~~P~~V~~N~~A~~ : 177
G. soli : T~~S~~T~~S~~A~~I~~V~~V~~M~~V~~Q~~G~~I~~N~~T~~F~~I~~R~~Q~~L~~N-~~A~~T~~Q~~S~~Y~~D~~R~~I~~G~~D~~S~~D~~E~~K~~A~~R~~A~~G~~L~~I~~A~~G~~A~~D~~Q~~I~~R~~G~~A~~L~~G~~D~~R~~T~~P~~T~~D~~V~~G~~D~~P~~A~~R~~T : 144

N. seriolae : V~~V~~N~~A~~A~~R~~S~~I~~A~~A~~E~~I~~R~~K~~M~~S~~G~~G~~S~~S~~V~~A~~P~~I~~N~~D~~A~~S~~K~~K~~V~~N~~D~~A~~L~~T~~A~~V~~R~~N~~A~~C~~P~~G~~K----- : 185
N. concava : V~~V~~T~~A~~A~~R~~A~~I~~A~~A~~E~~I~~R~~K~~L~~S~~S~~G~~A~~S~~V~~A~~P~~I~~N~~D~~A~~S~~K~~K~~V~~N~~D~~A~~L~~T~~A~~V~~R~~N~~A~~C~~P~~A~~K----- : 185
N. brasiliensis : V~~V~~N~~A~~A~~R~~A~~I~~S~~A~~E~~T~~R~~K~~M~~T~~Y~~T~~A~~P~~V~~G~~P~~I~~N~~D~~A~~S~~R~~R~~V~~N~~D~~A~~R~~N~~A~~V~~R~~D~~A~~C~~P~~K~~R----- : 185
M. rhodesia : V~~V~~D~~A~~A~~R~~R~~I~~A~~V~~A~~I~~A~~G~~N~~Y~~G~~P~~D~~E~~F~~N~~A~~I~~T~~K~~L~~N~~D~~T~~K~~T~~S~~A~~L~~N~~I~~C~~D~~A~~A~~Y~~----- : 191
M. marinum : V~~T~~D~~A~~A~~R~~A~~V~~A~~N~~A~~I~~G~~T~~H~~A~~P~~T~~G~~E~~F~~N~~R~~R~~V~~D~~Q~~L~~N~~D~~T~~K~~T~~K~~A~~L~~K~~I~~C~~M~~A~~S~~Y----- : 200
S. piniformis : V~~A~~G~~A~~A~~R~~E~~L~~A~~T~~A~~A~~D~~Q~~M~~Q~~D---A~~V~~Q~~A~~V~~N~~Q~~A~~K~~E~~R~~F~~N~~D~~S~~L~~E~~A~~V~~R~~K~~G~~C~~D~~----- : 188
R. globerulus : L~~A~~D~~N~~L~~R~~S~~I~~A~~G~~V~~I~~K~~R~~D~~H~~S~~P~~D~~E~~I~~N~~S~~I~~T~~D~~T~~T~~N~~S~~I~~R~~D~~S~~I~~R~~T~~E~~C~~G~~A~~L~~----- : 188
R. opacus : V~~A~~D~~N~~Y~~R~~E~~L~~A~~A~~A~~V~~D~~S~~G~~Q~~R~~G~~D~~I~~N~~T~~I~~A~~S~~R~~G~~D~~E~~L~~S~~D~~S~~I~~R~~A~~A~~C~~P~~T~~S----- : 178
G. polyisoprenivorans : F~~L~~T~~S~~S~~G~~R~~I~~G~~D~~A~~I~~G-R~~R~~E~~L~~V~~G~~I~~N~~P~~I~~A~~D~~T~~W~~T~~R~~D~~K~~Q~~S~~V~~L~~A~~V~~C~~A~~T~~Y~~L~~P~~T~~P~~P~~G~~L~~A~~P-----T~~T~~T~~G~~A~~R~~P~~P~~G : 236
G. soli : F~~L~~N~~T~~T~~G~~E~~I~~G~~A~~L~~I~~G-K~~R~~E~~L~~G~~G~~I~~N~~P~~I~~S~~D~~R~~W~~T~~R~~E~~K~~N~~A~~V~~L~~A~~V~~C~~G~~K~~Y~~R~~P~~L~~P~~P~~A~~T~~P~~S~~D~~Q~~G~~T~~A~~P~~S~~S~~G~~A~~V~~P~~P~~P : 208

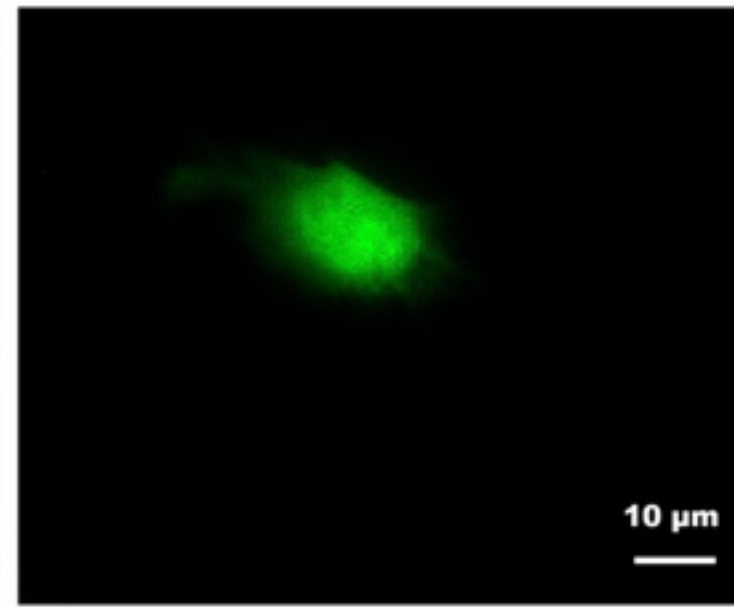
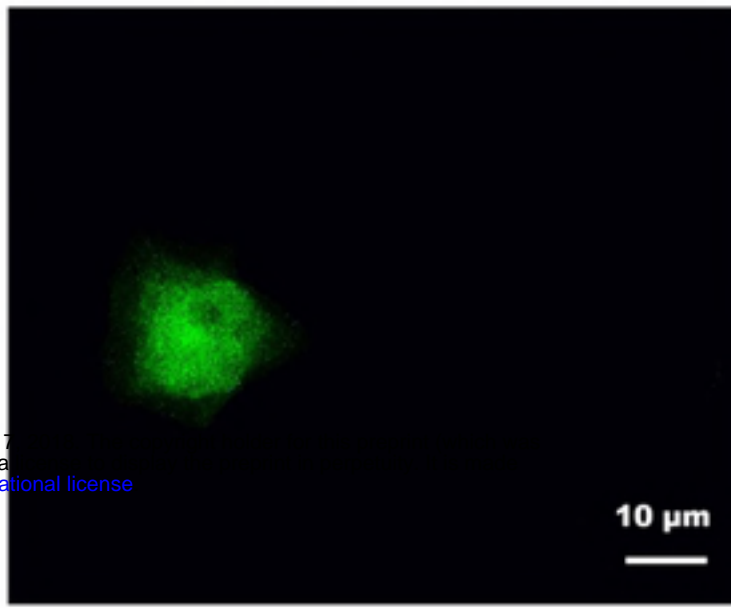
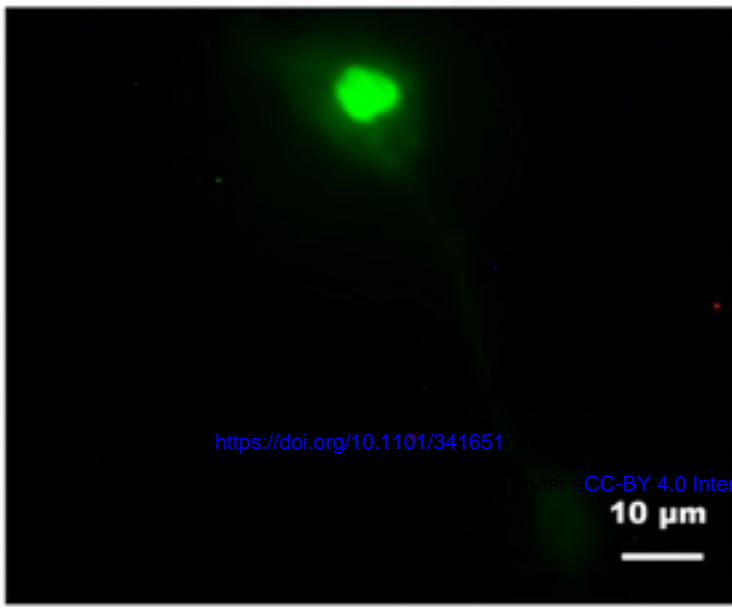


pEGFP-3141

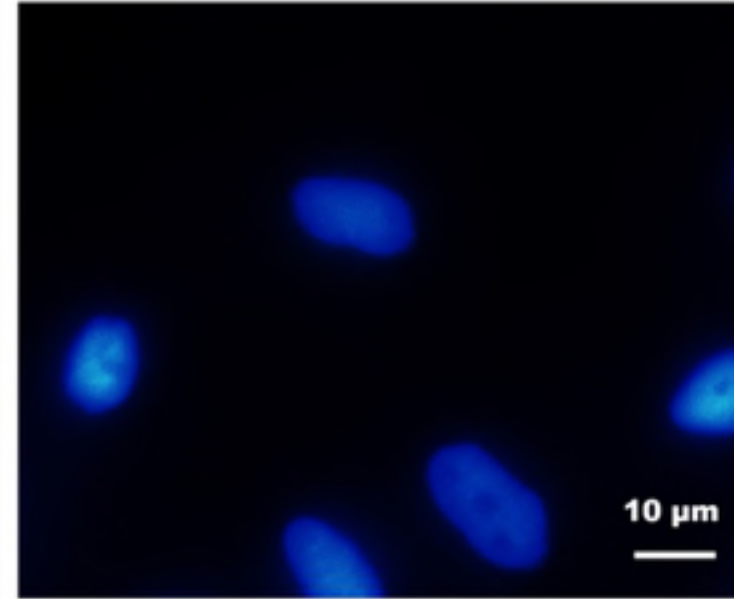
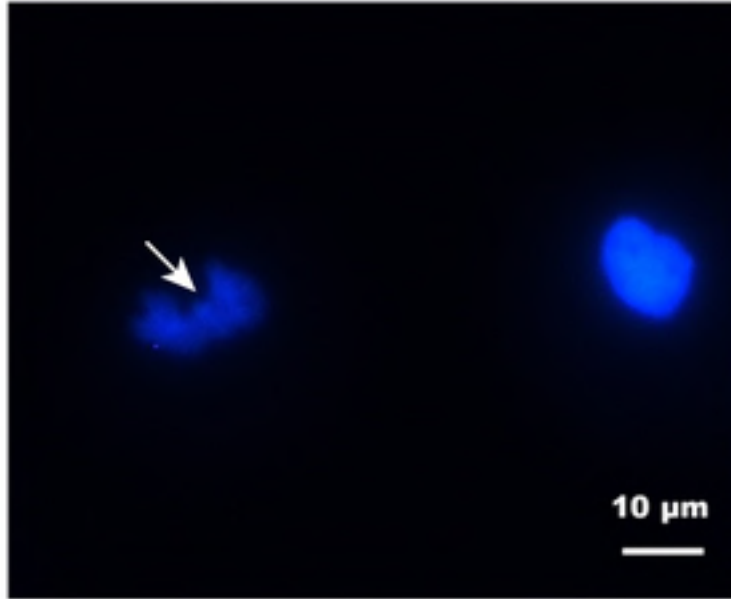
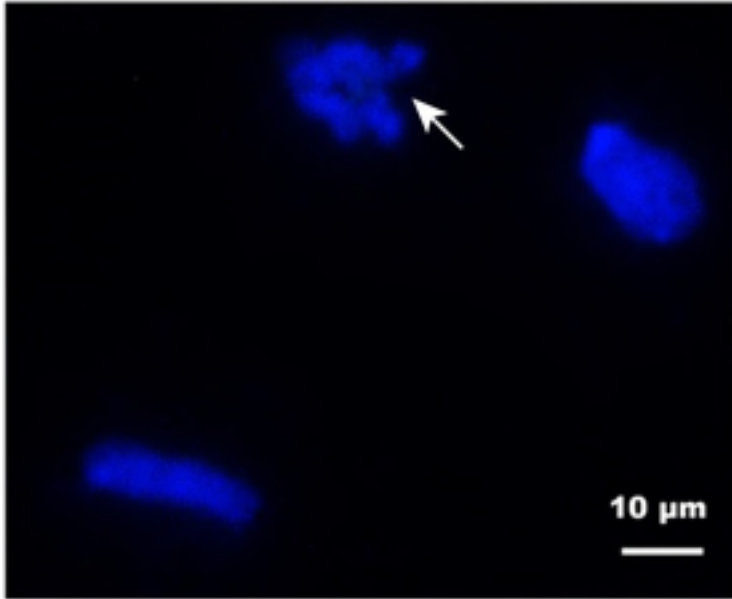
pEGFP-3141 Δ sig

pEGFP-N1

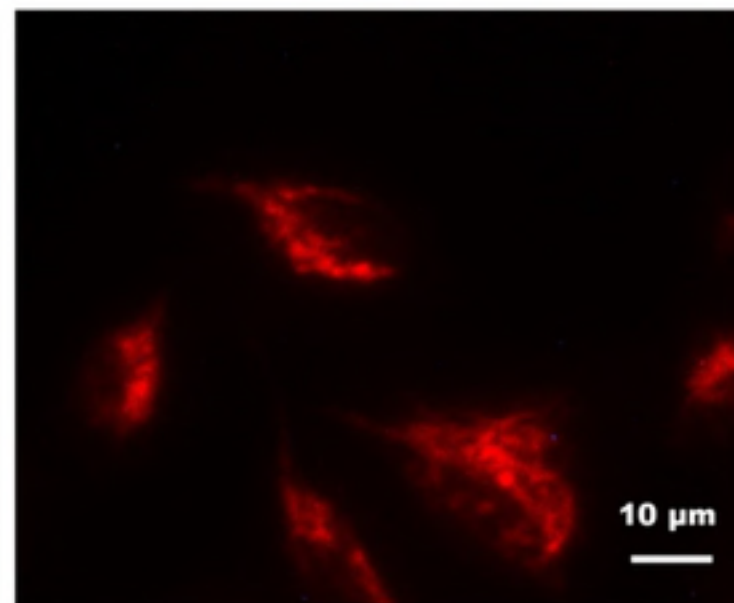
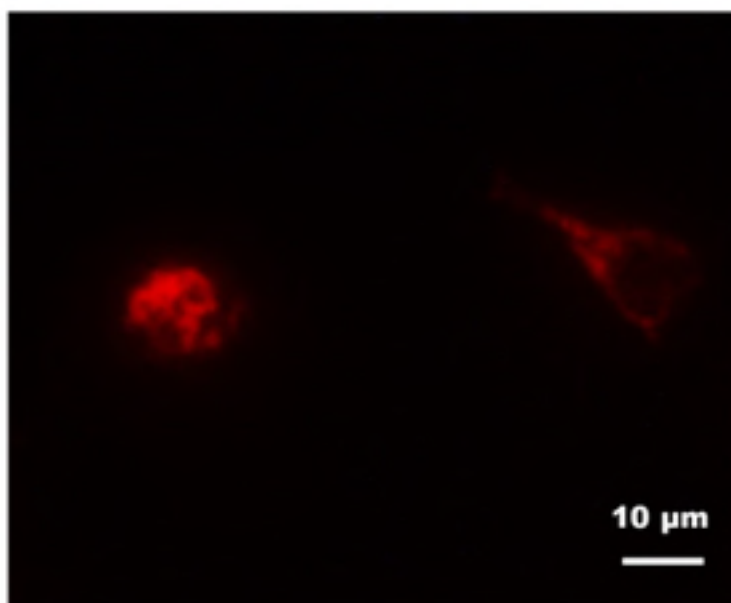
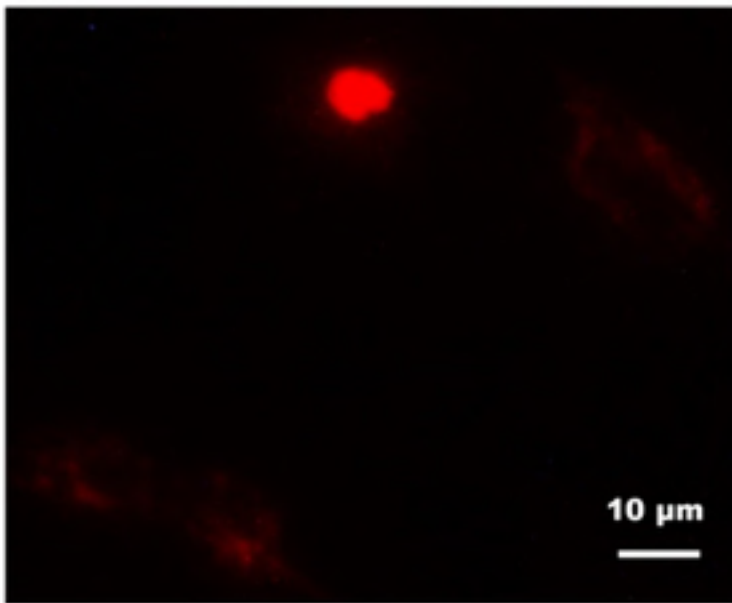
GFP



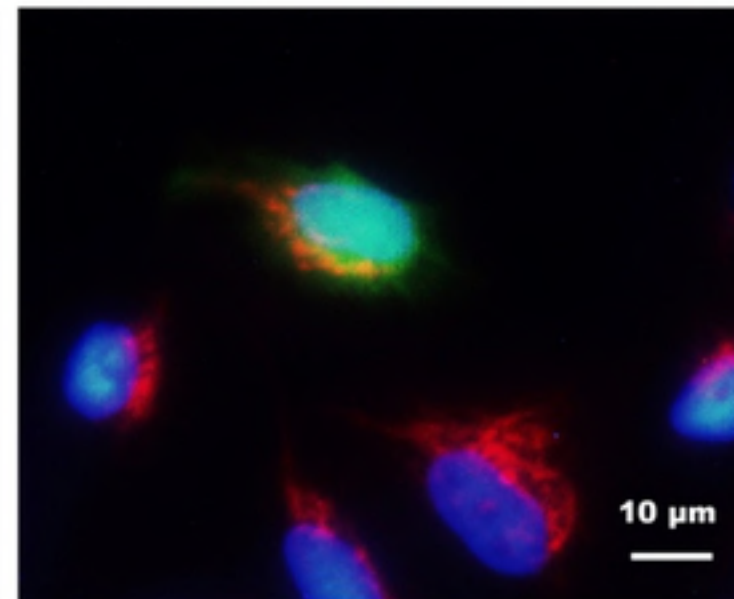
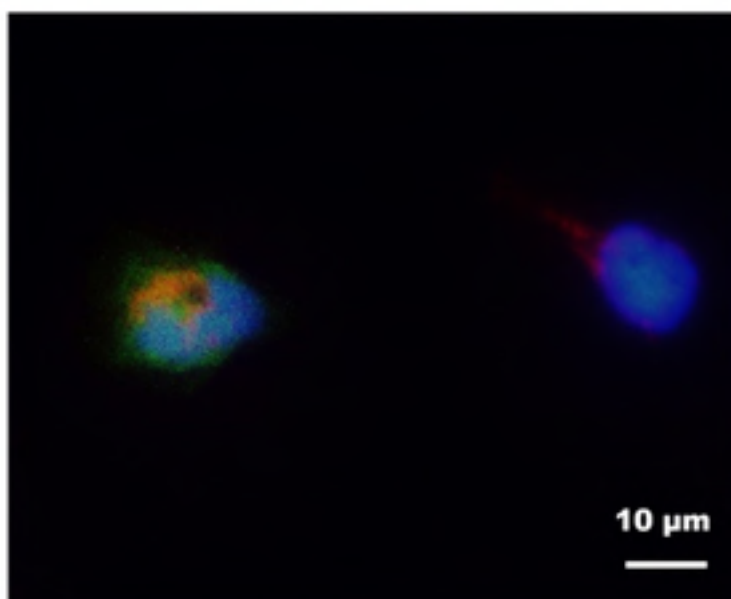
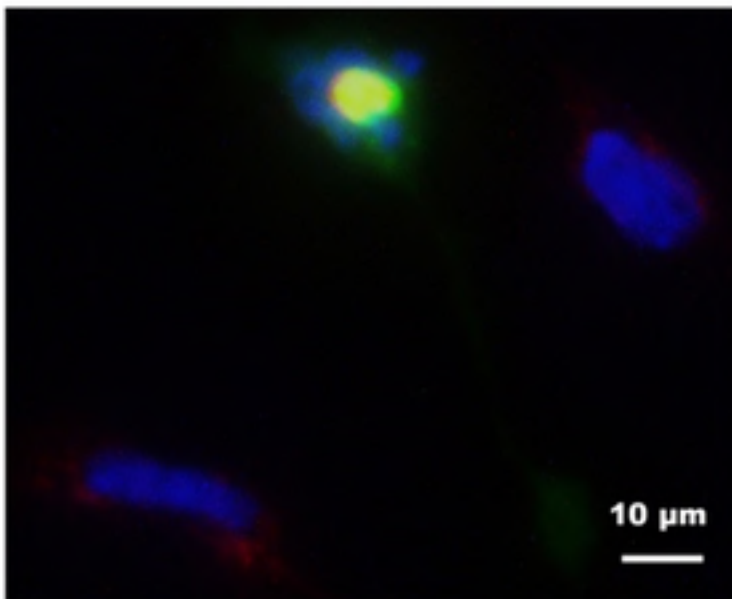
DAPI



Mito Tracker Red



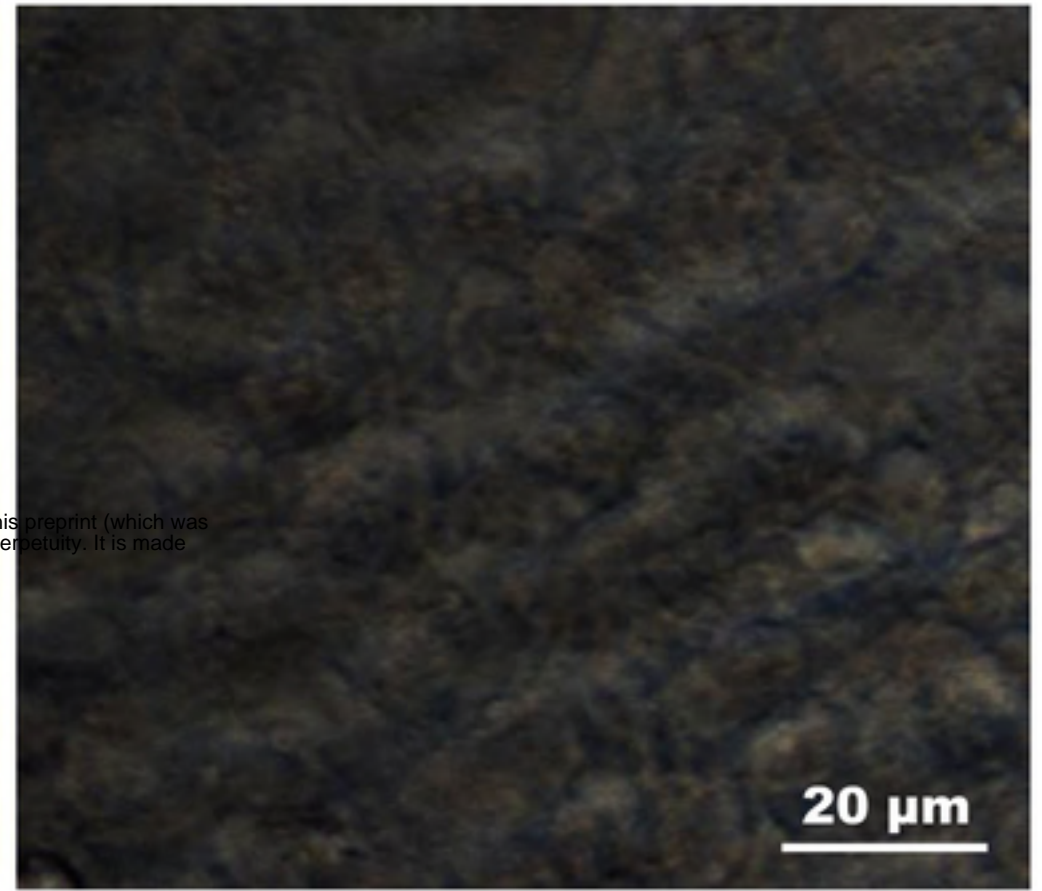
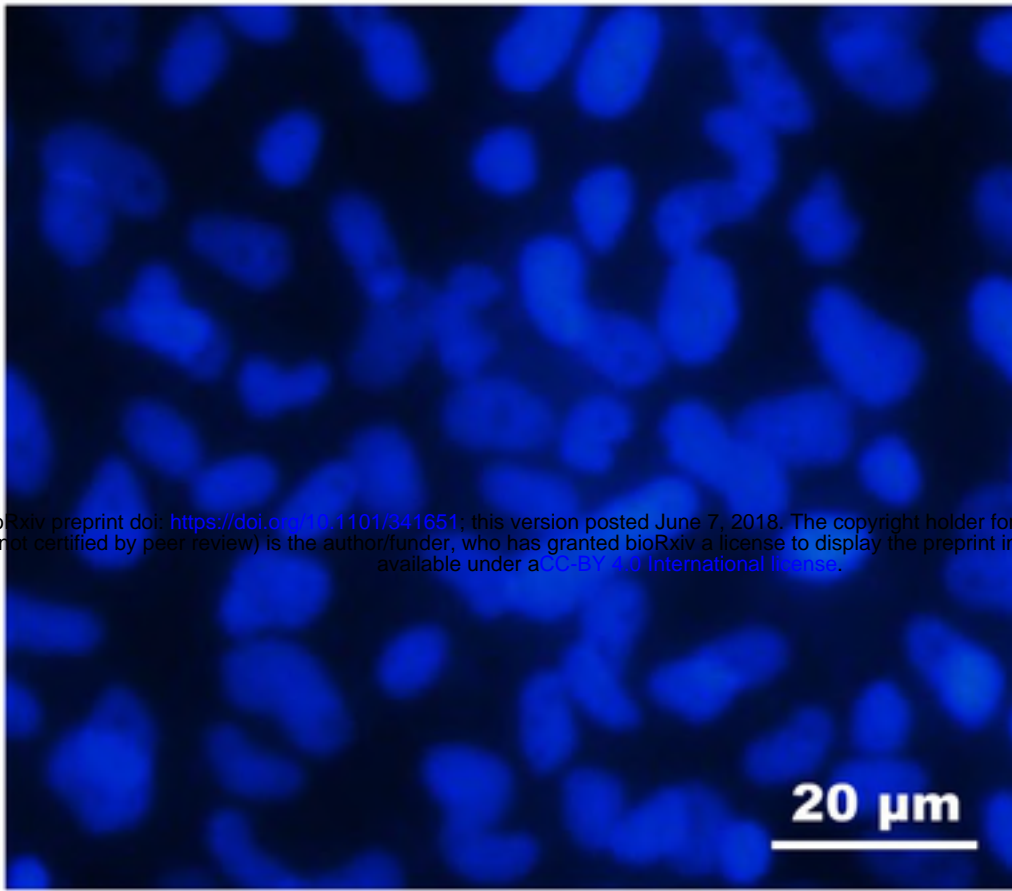
Merge



Fluorescent light

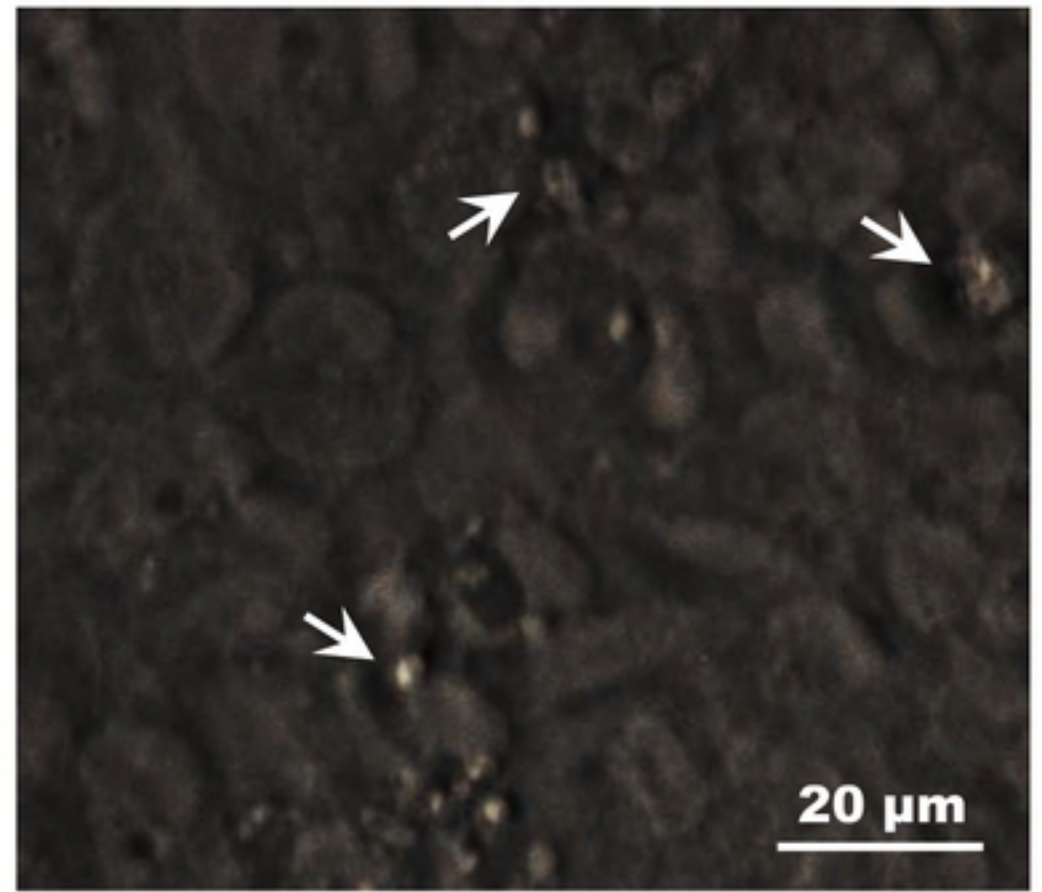
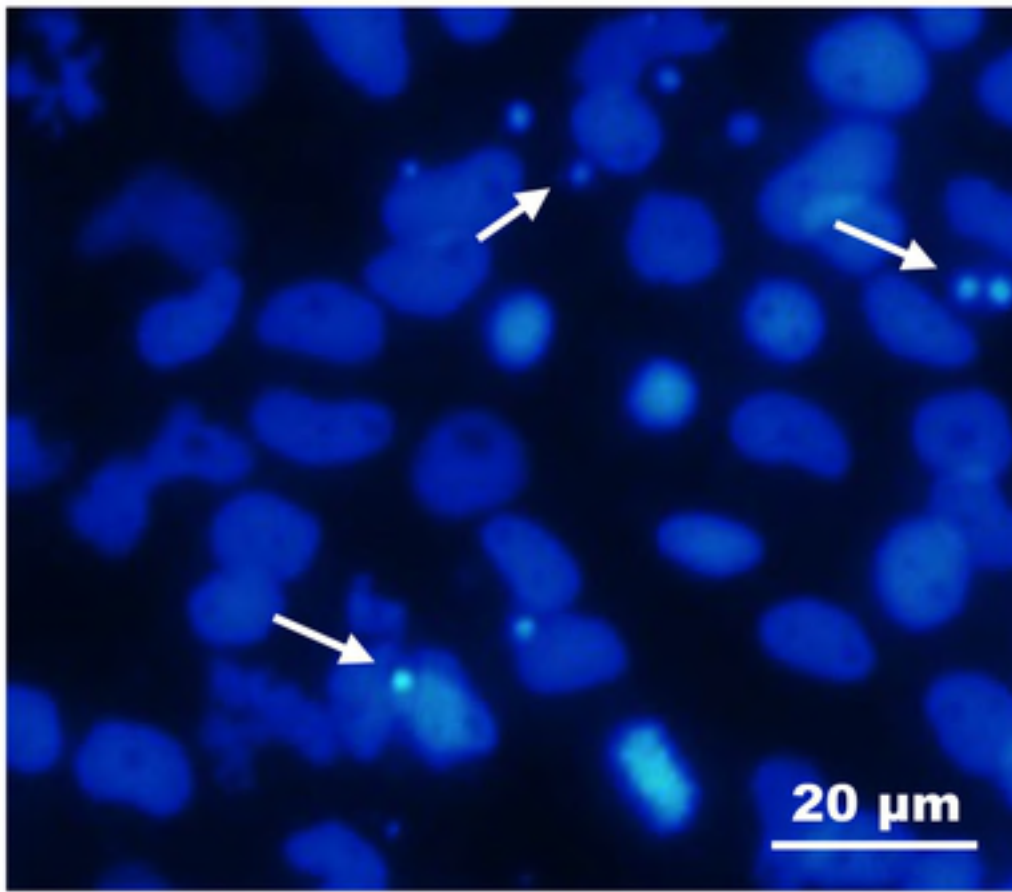
White light

pcDNA



bioRxiv preprint doi: <https://doi.org/10.1101/341651>; this version posted June 7, 2018. The copyright holder for this preprint (which was not certified by peer review) is the author/funder, who has granted bioRxiv a license to display the preprint in perpetuity. It is made available under aCC-BY 4.0 International license.

pcDNA-3141 Δ sig



pcDNA-3141

